Biomedicine & Pharmacotherapy 192 (2025) 118668

Contents lists available at ScienceDirect

Biomedicine & Pharmacotherapy

journal homepage: www.elsevier.com/locate/biopha

Transcriptomic profiling of organoids derived from malignant effusions uncovers lncRNA *MEG3* and target genes potentially involved in platinum resistance in serous ovarian carcinoma

Naiade Calanca [a,b], Claudia Aparecida Rainho [b], Debora Kazumi Maeda [a,b], Luiza Côrtes [a,c], Rolando André Rios Villacis [a,d], Daniela Bizinelli [e], Hellen Kuasne [f], Mads Malik Aagaard [a], Lars Ulrik Fokdal [g,h], Karina Dahl Steffensen [g,h], Lars Henrik Jensen [g,h,1], Silvia Regina Rogatto [a,c,h,*,1]

[a] Department of Clinical Genetics, University Hospital of Southern Denmark, Vejle 7100, Denmark
[b] Department of Chemical and Biological Sciences, Institute of Biosciences, São Paulo State University (UNESP), Botucatu, SP 18618-689, Brazil
[c] Botucatu Medical School Hospital, São Paulo State University (UNESP), Botucatu, SP 18618-687, Brazil
[d] Department of Genetics and Morphology, University of Brasília (UnB), Brasília, DF 70910-900, Brazil
[e] Interunit Graduate Program in Bioinformatics, Institute of Chemistry, University of São Paulo (USP), São Paulo, SP 05508-090, Brazil
[f] Rosalind and Morris Goodman Cancer Institute, McGill University, Montreal, QC H3A 1A3, Canada
[g] Department of Oncology, University Hospital of Southern Denmark, Vejle 7100, Denmark
[h] Institute of Regional Health Research, University of Southern Denmark, Odense 5000, Denmark

ARTICLE INFO

Keywords:
Serous ovarian carcinoma
Tumor-derived organoids
Long noncoding RNAs
Epigenetic drugs
MEG3

ABSTRACT

Serous ovarian carcinoma (SOC) is an aggressive disease, characterized by advanced-stage tumors that are often associated with relapse and poor outcomes. Although platinum-based chemotherapy is a cornerstone of the treatment, most of the relapsed tumors become resistant to these agents. We explored organoids derived from SOC malignant effusions to identify targets actionable by epigenetic drugs (epi-drugs) to enhance platinum response. Tumor-derived organoids (TDOs) were established using malignant effusions of SOC patients. Histological and transcriptomic (RNA-Seq) characterization (18 TDOs versus 7 normal ovarian samples) was performed, followed by cross-validation with external RNA-Seq datasets (337 SOC samples, 4 TDOs, and 180 normal tissues). Predicted interactions between long noncoding RNAs (lncRNAs) and epigenetic effectors were investigated. We selected the epi-drugs decitabine and tazemetostat, whose targets were overexpressed in SOC, to treat carboplatin-resistant SOC cell lines and TDOs. Subsequently, these models were challenged with carboplatin. Twelve lncRNAs and 168 protein-coding genes differentially expressed were involved in epigenetic regulation. Abnormal expression levels of lncRNA *MEG3* and epigenetic effectors *DNMT3B* and *EZH2* were confirmed in external datasets. Increased carboplatin sensitivity and *MEG3* upregulation were observed after treating the cell lines and TDOs with epi-drugs. Altogether, our findings provide novel insights into using organoids derived from malignant effusions as preclinical models and hint at potential targets for overcoming platinum resistance in SOC.

1. Introduction

Ovarian cancer (OC) is characterized by histological and molecular heterogeneity, which affects clinical outcomes [1]. Serous ovarian carcinoma (SOC), the most common and deadly histological type of OC, is an aggressive disease associated with relapse, resistance to

* Correspondence to: Botucatu Medical School Hospital, São Paulo State University (UNESP), Botucatu, SP 18618-687, Brazil.
E-mail addresses: naiade.calanca@unesp.br (N. Calanca), claudia.rainho@unesp.br (C.A. Rainho), debora.maeda@unesp.br (D.K. Maeda), luiza.cortes@unesp.br (L. Côrtes), rolando.andre@unb.br (R.A.R. Villacis), daniela.bizinelli@usp.br (D. Bizinelli), hellen.kuasne@mcgill.ca (H. Kuasne), Mads.Jorgensen@rsyd.dk (M.M. Aagaard), lars.ulrik.fokdal@rsyd.dk (L.U. Fokdal), Karina.Dahl.Steffensen@rsyd.dk (K.D. Steffensen), Lars.Henrik.Jensen@rsyd.dk (L.H. Jensen), silvia.regina.rogatto@rsyd.dk, silvia.rogatto@unesp.br (S.R. Rogatto).
[1] These authors contributed equally.

https://doi.org/10.1016/j.biopha.2025.118668
Received 7 August 2025; Received in revised form 7 October 2025; Accepted 17 October 2025
Available online 22 October 2025

chemotherapy, and poor prognosis (approximately 30 % 5-year survival) [2]. SOC comprises high- and low-grade subtypes, in which high-grade is the most frequently diagnosed and is responsible for 70–80 % of deaths due to the disease [3]. Patients with newly diagnosed OC are treated with chemotherapy regimens, usually combining platinum-based agents (cisplatin or carboplatin) with taxanes (e.g., paclitaxel) [4]. Although high-grade SOC (HGSOC) initially responds to chemotherapy, 80–90 % of advanced-stage tumors are estimated to become resistant [3]. The treatment of choice for low-grade SOC (LGSOC) is based on primary debulking surgery due to its lack of responsiveness to chemotherapy [5].

Transcriptomic and epigenetic signatures (e.g., noncoding RNA expression, histone modifications, and DNA methylation) have been associated with clinical outcomes [6]. Furthermore, epigenetic aberrations in OC tissues, such as DNA hypermethylation and repressive histone marks, are responsible for silencing genes associated with chemotherapy response [7]. Thus, harnessing epigenetic changes is a promising strategy to overcome chemoresistance. Additionally, a combination of drugs targeting different molecular alterations may be more effective than conventional approaches in treating this heterogeneous disease.

Long noncoding RNAs (lncRNAs) are transcripts longer than 200 nucleotides that are not usually translated into proteins and can modulate gene expression by directly interacting with proteins of the epigenetic machinery, such as histone modifying and chromatin remodeling complexes [8]. Aberrant lncRNA expression has been implicated in OC progression and response to therapy [9]. For instance, the expression levels of five lncRNAs were positively associated with FIGO (International Federation of Gynaecology and Obstetrics) stage and lymph node metastasis, while other 62 lncRNAs were differentially expressed in cisplatin-resistant OC [10,11]. As lncRNAs cooperate with epigenetic effectors in fine-tuning gene expression, the dysregulation of these transcripts may interfere with the course of OC by influencing the dynamic epigenetic control.

Organoids are three-dimensional (3D) multicellular *in vitro* tissue constructs that recapitulate the molecular factors and other aspects of their corresponding *in vivo* organs, capturing the complexity of development, homeostasis, and pathogenesis in more detail than two-dimensional monolayer cultures [12,13]. Malignant effusions from OC patients are promising samples for generating tumor-derived organoids (TDOs) since they contain tumor and non-tumor cells, such as fibroblasts, adipocytes, mesothelial, endothelial, and inflammatory cells [14]. OC is the most common cancer type associated with ascites, which is present in more than one-third of patients, and the sixth cancer type causing pleural effusion [15,16]. These malignant fluids are repeatedly drained during the disease course to alleviate symptoms, making them an excellent material for studying the tumor progression and the resistance to therapy over time. Previous studies have demonstrated the suitability of HGSOC ascites for *in vitro* drug sensitivity testing and for identifying biomarkers useful for clinical resistance prediction [17,18]. A recent study utilized organoids derived from the ascites of SOC patients to assess the potential of epigenetic drugs (epi-drugs) in improving the response to immunotherapy [19].

In this study, we generated TDOs from malignant effusions of SOC patients to characterize the expression of lncRNAs and their interplay with the epigenetic machinery. By analyzing the transcriptome of organoids derived from SOC effusions and conducting drug tests, we pinpointed epigenetic regulators that exhibited abnormal expression levels and could be targeted with epi-drugs. Our experimental model and future research may contribute to the development of personalized drug screening platforms for SOC patients.

2. Materials and methods

2.1. Patients

Twenty-one patients with SOC who presented malignant effusions (ascites or pleural effusion) and were referred to the University Hospital of Southern Denmark, Vejle, DK (February 2020 to June 2022) for thoracocentesis or paracentesis were eligible to participate in the study. All patients signed an informed consent form, and those with clinically relevant medical conditions (e.g., uncontrolled hypertension and heart disease) that could impair the study results were excluded. Eight out of 21 SOC samples and seven normal ovarian samples were obtained from a previous study conducted by our group [20]. The normal samples were collected from individuals who either underwent surgery for cysts (three cases) or had hysterectomies (four cases). All cases underwent histopathological analysis and were categorized as normal ovarian tissues. Follow-ups over 10 years confirmed that all patients remained healthy. For two SOC patients, more than one sample was collected. Among the SOC cases, two were from chemotherapy-naïve patients (T4 and T5), while the others had received systemic treatment before the sample was taken. Clinical data of SOC patients (11 high-grade and 4 low-grade SOCs) were retrieved from electronic medical records (Table 1). In the last follow-up (April 2024), all patients had died from the disease.

2.2. Tumor-derived organoids (TDOs) establishment and maintenance

Malignant effusion fluids were collected from 21 patients with SOC and processed immediately after drainage. TDOs were established following a protocol previously described by our group [20]. Briefly, cells were washed in medium and resuspended on StemPro™ hESC SFM growth full medium (Dulbecco's modified Eagle medium [DMEM]/F-12, GlutaMAX™, 25 % bovine serum albumin, and StemPro® hESC Supplement) (Thermo Fisher Scientific, Waltham, MA, USA) supplemented, at final concentration, with 8 ng/mL human fibroblast growth factor (FGF)-basic (Thermo Fisher Scientific), 100 μM 2-mercaptoethanol (Thermo Fisher Scientific), 200 U/mL penicillin, 200 μg/mL streptomycin (Sigma-Aldrich, St. Louis, MO, USA), 100 μg/mL gentamycin (Sigma-Aldrich), 2.5 μg/mL amphotericin B (Sigma-Aldrich), and mixed with Matrigel® Basement Membrane Matrix (final concentration of Matrigel at 50 %; Corning Inc., Corning, NY, USA). Cell suspension was solidified on pre-warmed 24-well culture plates at 37 °C for 30 min. After incubation, medium and supplements were added to each well, and plates were incubated at 37 °C, 5 % CO_2. The medium was changed every 2–3 days. TDOs developed within 1–4 weeks and were harvested using Cell Recovery Solution (Corning Inc.), according to the manufacturer's instructions. Pellets were used for RNA extraction.

2.3. Histological characterization

Primary SOCs paired with corresponding TDOs (6–15 days) were fixed and processed for histological analysis using automated protocols (Tissue-Teck VIP 6AI Tissue Processor, Sakura Finetek, Japan). Representative sections of formalin-fixed and paraffin-embedded OC tissues and TDOs were stained with hematoxylin and eosin (H&E) and compared. The expression of protein markers PAX8, CK7, and TP53, used for characterizing organoid-tissue pairs in previous studies [21,22], was evaluated by immunohistochemistry assays using the Benchmark Ultra automated instrument (Ventana Medical Systems, Roche, Tucson, AZ, USA) or Dako Omnis (Agilent Technologies, Santa Clara, CA, USA).

2.4. RNA isolation, sequencing, and data analysis

For RNA sequencing (RNA-Seq), total RNA was isolated using the RNeasy Mini Kit (Qiagen, Valencia, CA, USA), following the manufacturer's recommendations. RNA purity and quantity were measured using the Nanodrop spectrophotometer (Thermo Fisher Scientific,

Table 1
Clinical and treatment characteristics of serous ovarian cancer patients included in the study.

Case	Age at diagnosis (years)	Source	FIGO Stage	Neoadjuvant first line chemotherapy	Maintenance therapy after first line	Treatment (cycles)	Last treatment
HIGH-GRADE SEROUS OVARIAN CARCINOMA							
T1	69	Pleural effusion	IV	No - operated at diagnosis primary debulking surgery	Bevacizumab	Paclitaxel/Carboplatin + Bevacizumab from sixth cycle (6)	Carboplatin
T2	52	Ascites	IV	Paclitaxel/Carboplatin	Bevacizumab	Paclitaxel/Carboplatin + Bevacizumab (6)	-
T4[a]	64	Ascites	IIIC	No - operated at diagnosis primary debulking surgery	No	Paclitaxel/Carboplatin (1)	Carboplatin/ Paclitaxel
T5[b]	71	Ascites	IV	No	No	Untreated	-
T7[c]	65	Ascites	IV	Paclitaxel/Carboplatin	No	Paclitaxel/Carboplatin (8)	-
T8	37	Pleural effusion	IV	Paclitaxel/Carboplatin (6)	Bevacizumab	Liposomal Doxorubicin (6) Carboplatin (4) Topotecan (3)	Topotecan
T9	69	Pleural effusion	IIIB	Paclitaxel/Carboplatin (changes to pure palliative after the first 3 cycles)	Bevacizumab	Paclitaxel/Carboplatin (6) Treosulfan (2)	Treosulfan
T10	75	Pleural effusion	IIIC	No - operated at diagnosis primary debulking surgery	No	Paclitaxel/Carboplatin (6) Liposomal Doxorubicin/ Carboplatin (5)	Carboplatin
T11	76	Ascites	IIIC	Paclitaxel/Carboplatin (changes to pure palliative after the first 3 cycles)	No	Paclitaxel/Carboplatin (5)	Carboplatin
T12	70	Ascites	IV	Paclitaxel/Carboplatin	Bevacizumab followed by Olaparib	Paclitaxel/Carboplatin (6) Olaparib (6) Liposomal Doxorubicin (2) Topotecan (6) Treosulfan (2)	Treosulfan
T14	83	Ascites	IIB	No - operated at diagnosis primary debulking surgery	No	Carboplatin (6)	Carboplatin
LOW-GRADE SEROUS OVARIAN CARCINOMA							
T3	60	Pleural effusion	IIC	No - operated at diagnosis primary debulking surgery	No	Paclitaxel/Carboplatin (6) Carboplatin (6) Carboplatin (6) Carboplatin (6) Bevacizumab monotherapy (6)	Carboplatin
T6	53	Pleural effusion	IIIC	No - operated at diagnosis primary debulking surgery	Bevacizumab	Bevacizumab + Tocotrienol (9)	Topotecan
T13	76	Pleural effusion	IV	Paclitaxel/Carboplatin	Bevacizumab	Carboplatin (3)	Bevacizumab
T15[c]	58	Ascites	IV	Paclitaxel/Carboplatin (changes to pure palliative after the first 3 cycles)	No	Paclitaxel/Carboplatin (8) Liposomal Doxorubicin (4) Topotecan (4) Paclitaxel weekly (28) Trametinib Carboplatin (2) Letrozole (oral daily)	Letrozole

[a] Patient T4: diagnosed with high-grade serous ovarian carcinoma with a sarcomatous component (carcinosarcoma).
[b] Patient T5 did not undergo surgery or chemotherapy due to poor performance status.
[c] Patients sampled more than once. FIGO: International Federation of Gynecology and Obstetrics.

Waltham, MA, USA), and its integrity was evaluated using a 4200 TapeStation RNA screen (RNA ScreenTape; Agilent, Santa Clara, CA, USA).

The cDNA libraries were prepared using 100 ng total RNA with the Illumina Stranded Total RNA Prep, Ligation with Ribo-Zero Plus kit (Illumina, San Diego, CA, USA), according to the manufacturer's instructions. IDT for Illumina RNA UD Indexes Set A was added to multiplex the samples, and the paired-end sequencing was performed on Illumina NovaSeq 6000 System (2 $\times$150 bp). RNA-Seq data quality control was conducted using MultiQC [23]. The reads were aligned to the reference genome assembly GRCh38 (Genome Reference Consortium Human Build 38) using the Spliced Transcripts Alignment to a Reference (STAR) software [24] and quantified for each Ensembl gene ID using featureCounts [25]. Only genes with read counts ≥ 1 in at least 90 % of samples were retained (23,324 genes out of 60,660). Gene annotation was performed using biomaRt R package (v. 2.50.3) [26], and Ensembl IDs without corresponding Entrez Gene ID, gene symbol, or gene type were removed. The final count matrix comprised 23,275 Ensembl IDs (i.e., genes). Read count normalization and transformation were performed with the DESeq2 R package (v. 1.34.0) [27]. Differential gene expression analysis between TDOs and normal ovarian tissue samples was conducted with the limma R package (v. 3.50.3) [28]. Differentially expressed genes (DEGs) were identified considering *p*-value adjusted to control false discovery rate (FDR) and fold-change (FC) criteria (FDR$<$0.05 and $|FC|\geq 2$).

For two patients sampled more than once (T7 and T15), the normalized expression levels of annotated genes were compared between the TDOs derived from the same patient based on variance. We selected genes with variance ≥ 5 across samples to identify the most variable during SOC progression.

2.5. External RNA-Seq data processing

Raw count data of SOC patients (N = 337) were retrieved from The Cancer Genome Atlas - Ovarian Cancer project (TCGA-OV) using the TCGAbiolinks Bioconductor/R package (v. 2.25.2) [29]. Clinical data of these patients were downloaded from Xena Browser (http://xena.ucsc.edu/) [30]. Raw count data of healthy ovarian tissue samples were obtained from the Genotype-Tissue Expression (GTEx) Portal (GTEx Analysis Release V8) (N = 180). These datasets (tumor and normal) were integrated into a single matrix and analyzed following the same protocol used in our internal RNA-Seq data. The Ensembl IDs (genes) shared by the TCGA and GTEx data were filtered to keep only those with read count ≥ 1 in at least 90 % of the samples and then annotated with the biomaRt package (v. 2.50.3) [26]. The final count matrix consisted of 21,834 Ensembl IDs (genes). Next, data normalization and transformation were performed according to the DESeq2 package protocol (v. 1.34.0) [27]. Differences in global gene expression between normal and tumor samples were analyzed using the limma package (v. 3.50.3) [28].

Previously published RNA-Seq data from TDOs (culture day 6) derived from malignant effusions from four patients with HGSOC were obtained upon request [31]. This dataset was integrated with ours and processed as described earlier. The batch effect between the two datasets was removed using the ComBat_seq function from the sva package (v. 3.42.0) [32]. Global gene expression differences between TDOs (internal, N = 15, and external TDOs, N = 4) and normal samples (N = 7) were analyzed.

2.6. Identification of epigenetic regulators

The differentially expressed lncRNAs and protein-coding genes (PCGs) identified in our TDO samples were filtered for epigenetic regulators according to the EpiFactors database (v. 2.0; https://epifactors.autosome.org/) [33]. Epigenetic regulators included lncRNAs involved in recruiting or sequestering chromatin remodelers, histone modifiers, DNA modifiers, transcription factors, and splicing factors, modulating protein functions, chromatin looping, promoter switching, transcription machinery interference, and RNA or protein binding. We also included PCGs involved in chromatin remodeling, histone and DNA modification, and protein scaffold formation. The DEGs associated with epigenetic regulation were selected for interaction analysis using the ncRNA Functional Annotation Server (ncFANs) database (v. 2.0; http://ncfans.gene.ac/) [34] considering lncRNA interactions with transcription factors and predicted interactions with RNA binding proteins (lncPro score = 80). lncPro scores the lncRNA–protein interaction pairs according to information about nucleotide and amino acid sequence [35]. The interactions were imported into Cytoscape software (v. 3.8.2) for visualization, and the network was analyzed using the CytoNCA plugin (v. 2.1.6) [36], which calculated the nodes' betweenness centrality. Betweenness values range between 0 and 1 and reveal how much each node influences the interactions of other nodes in the network [37].

2.7. OVCAR8 and Ovc316 cell lines culture

We conducted drug testing using two OC cell lines inherently resistant to carboplatin, namely OVCAR8 and Ovc316. These cell lines were donated by Wan Lam (University of British Columbia, Vancouver, Canada) and Robert Strauss (Danish Cancer Society, Copenhagen, Denmark), respectively. The cell lines were cultured in DMEM (Sigma Aldrich, St. Louis, MO, USA), supplemented with 10 % fetal bovine serum (Biological Industries, Beit HaEmek, Israel) and 1 % antibiotic-antimycotic (10,000 U/mL penicillin, 10 mg/mL streptomycin, and 25 µg/mL of Amphotericin B 100x) (Thermo Fisher Scientific, Waltham, MA, USA), at 37°C with 5 % CO_2. A PCR-based assay was used to investigate mycoplasma contamination. Cell counting was performed using the Countess II Automated Cell Counter (Thermo Fisher Scientific) based on Trypan blue exclusion.

2.8. Dose-response curves and IC_{50} determination

The epi-drugs decitabine (DAC) (Janssen-Cilag International NV, Beerse, Belgium) and tazemetostat (TAZ) (TargetMol Chemicals, Boston, MA, USA) were diluted in dimethyl sulfoxide (DMSO; Sigma Aldrich, St. Louis, MO, USA). The 50 % maximum growth inhibition (IC_{50}) was calculated using GraphPad Prism 7.0 (GraphPad Software, Boston, MA, USA). Approximately 5000 cells/well were seeded with supplemented media at the 96-well optical-bottom plate (Thermo Fisher Scientific, Waltham, MA, USA). After cell adhesion and starvation, DAC and TAZ were added, isolated, or combined at different concentrations (0.1, 0.25, 0.5, 1, 2.5, 5, and 10 µM). Cell viability was assessed after 24, 48, and 72 h of treatment using the CellTiter-Blue® Cell Viability Assay (Promega, Madison, WI, USA). The fluorescence values were recorded at 530/590 nm using the Synergy HT microplate reader (BioTek, Winooski, VT, USA). The experiments performed at each timepoint were repeated in triplicate using DMSO as a control, ensuring the thoroughness of the results.

2.9. Drug testing in cell lines and TDOs

Cells ($\sim 3 \times 10^5$) of both cell lines were exposed to DAC (1 µM) and TAZ (2.5 µM), isolated or combined, and to control (DMSO) for 96 h, followed by 24 h of recovery. Next, cells were treated with the Gibco trypsin-EDTA (Thermo Fisher Scientific, Waltham, MA, USA), and 5000 cells/well were seeded on the 96-well optical-bottom microplate. Carboplatin was added at 50 µM and 100 µM for 72 h of exposure, followed by cell viability assessment using the CellTiter-Blue® Cell Viability Assay (Promega, Madison, WI, USA) (Fig. S1A). The carboplatin dosage was determined according to a previous study of our group that included OVCAR8 and Ovc316 cell lines [38].

A similar strategy to the one described for cell lines was applied to TDOs derived from one patient (OV20231201PE) (Fig. S1B). After TDO generation, large organoids were dissociated using the Gibco TrypLE Express Enzyme (1x), phenol red (Thermo Fisher Scientific, Waltham, MA, USA), and filtered through a 40 µm cell strainer. Approximately 20,000 cells/well were seeded in 24-well Nunclon Sphera microplates (Thermo Fisher Scientific, Waltham, MA, USA). After 24 h of recovery, TDOs were treated with DAC and TAZ, isolated or in combination, at 0.5 and 2.5 µM, respectively, for 72 h. After recovering for 24 h, TDOs were exposed to carboplatin at 100 µM for 72 h. Cell viability was assessed, as described above. Luminescence was recorded using the Synergy HT microplate reader (BioTek, Winooski, VT, USA). Drug testing was performed in triplicate with at least two independent experiments.

2.10. RNA extraction and RT-qPCR

Total RNA was isolated from TDOs of patients sampled multiple times (T7 and T15) and from OVCAR8 and Ovc316 cell lines after DAC and/or TAZ treatment using the RNeasy Mini Kit (Qiagen, Valencia, CA, USA). cDNA was synthesized with the High-Capacity RNA-to-cDNA Kit (Thermo Fisher Scientific, Waltham, MA, USA). Expression analyses (RT-qPCR) were performed for *MEG3* (Hs00292028_m1) and *GUSB* (Hs00939627_m1) (Thermo Fisher Scientific, Waltham, MA, USA) in duplicates on QuantStudio 7 Flex Real-Time PCR System (Thermo Fisher Scientific, Waltham, MA, USA), using 10 ng of cDNA and TaqMan Fast Advanced Master Mix (Thermo Fisher Scientific, Waltham, MA, USA). Relative gene expression values were calculated using the $2^{-\Delta\Delta Ct}$ method [39]. Statistical analysis was carried out using the ANOVA *t*-test; a two-tailed test *p*-value < 0.05 was considered significant.

2.11. Statistical analyses and data visualization

Statistical analyses were performed using the R software (v. 4.1.0). Hierarchical clustering analyses based on Euclidean distance were conducted, and heatmaps were constructed using the R packages

ComplexHeatmap (v. 2.10.0) [40], cluster (v. 2.1.3), and RColorBrewer (v. 1.1–3). Gene set enrichment analysis (GSEA) was performed with the clusterProfiler R package (v. 4.8.3), and the ridge plots were generated using the enrichplot R package (v. 1.20.1). GSEA was run on the list of genes obtained from the differential expression analyses pre-ranked based on $-\log_{10}(p\text{-value})$ * sign (logFC). Pathways and ontologies enrichment was established using the DEGs from the internal dataset if the Benjamini–Hochberg adjusted p-value for the GSEA was < 0.05. The remaining graphs were performed using the ggpubr (v. 0.4.0) and ggplot2 (v. 3.3.6) R packages. Statistical analyses of the drug testing results were conducted in GraphPad Prism 10 (GraphPad Software, Boston, MA, USA), using ANOVA or Kruskal-Wallis tests (p-value < 0.05). A flowchart summarizing the study design and the analyses is depicted in Fig. S2.

3. Results

3.1. TDOs histologically resemble the corresponding primary SOC

We successfully generated 18 TDOs from 15 SOC patients (11 HGSOC

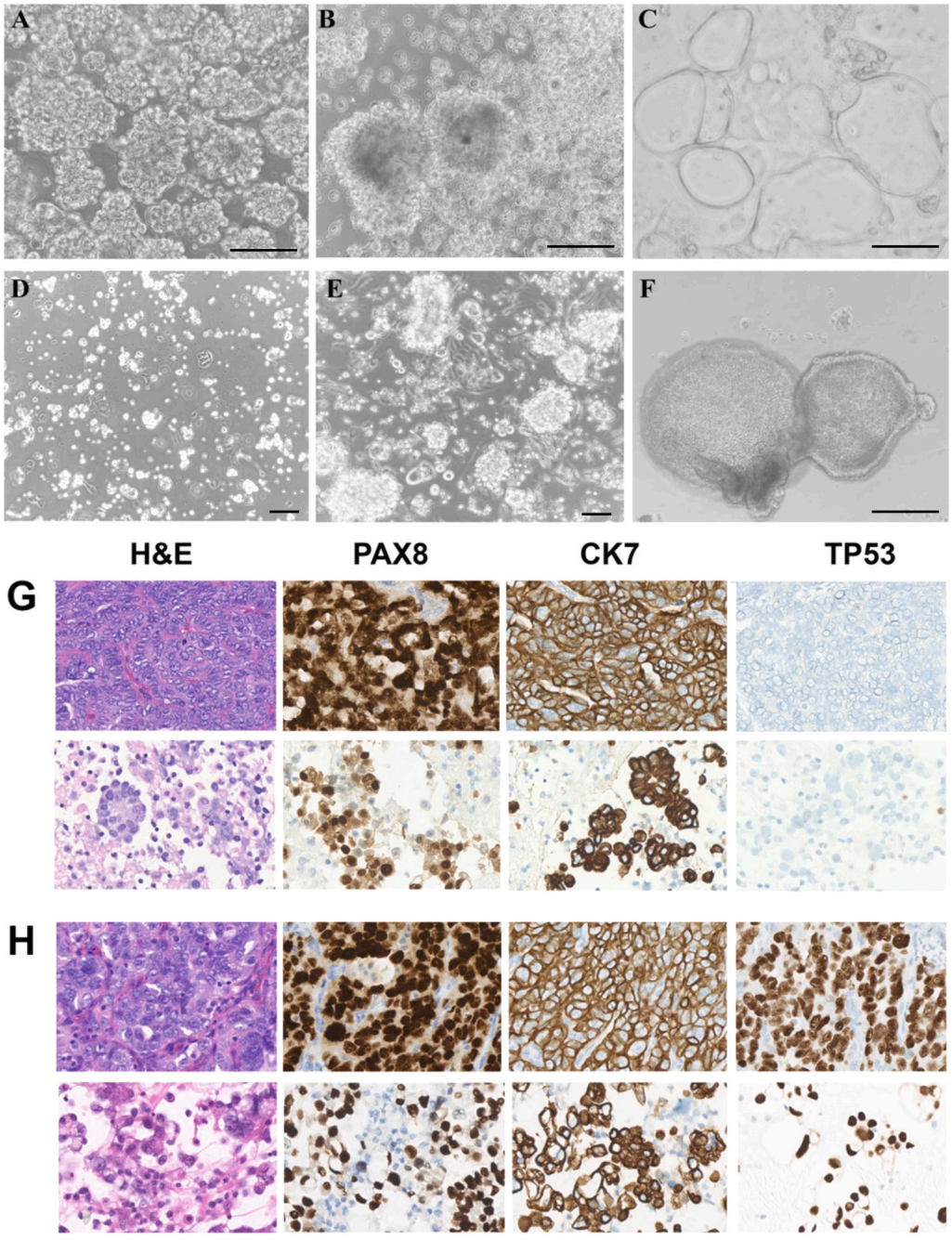

Fig. 1. Morphological and histological characterization of tumor-derived organoids (TDOs) generated using malignant effusions from serous ovarian carcinoma patients. (A-F) Examples of TDOs exhibiting different morphologies and degrees of cohesion. (A) and (D) TDOs on the first day of 3D cell culture (magnification 40x and 10x, respectively). (G-H) Representative high-grade serous ovarian carcinoma (HGSOC) tissue sections and their corresponding organoids were subjected to hematoxylin-eosin and immunohistochemical staining for histological comparison. The top and bottom panels in (G) and (H) show tumor tissues and organoids, respectively. The atypical cells of organoids derived from HGSOC and their corresponding primary tumors exhibit a similar expression of protein markers PAX8, CK7, and TP53. (G) Organoids derived from pleural effusion of HGSOC patients; (H) Organoids derived from ascites of HGSOC patients. Scale bars, 250 μm.

and 4 LGSOC). Although TDOs were obtained from six other patients, they showed a low proliferation rate and were excluded. Overall, we achieved a success rate of 71.4 % in TDO generation. Our patient cohort consisted of individuals with advanced diseases who underwent diverse therapeutic regimens, including two patients (T4 and T5) from whom we derived TDOs prior to treatment (Table 1). Samples were collected at various time points throughout the disease course. Among the SOC patients, 13 were diagnosed with FIGO stages III and IV. Two patients were sampled more than once: patient T7 (HGSOC) had two ascites samples collected with a 45-day interval; patient T15 (LGSOC) underwent ascites drainage three times, with intervals of 348 and 65 days. The SOC-derived organoids presented a wide range of morphologies, varying from cystic to dense, with different degrees of circularity and cellular cohesiveness (Fig. 1A-F). These histological patterns were not associated with patients' clinical characteristics or treatment responses. We compared the immunostaining patterns of PAX8, CK7, and TP53 in primary SOCs and their corresponding organoids. As we previously described, concordant protein expressions were verified for all biomarkers investigated (Fig. 1G, H) [20].

3.2. RNA-Seq data reveal lncRNAs with decreasing expression levels during the SOC course

The comparison between gene expression profiles of TDOs and normal ovarian tissue samples from our internal dataset revealed 7668 DEGs: 3586 upregulated and 4082 downregulated genes in TDOs. A total of 1428 DEGs corresponded to genes encoding lncRNAs (Table S1), 69 % (N = 983) with reduced expression levels, while 5241 were identified as PCGs, in which 55 % (N = 2881) showed increased expression levels. An unsupervised clustering analysis based on the profile of differentially expressed lncRNAs revealed two clusters that accurately separated TDOs and normal samples (Fig. 2A).

For two patients, one with HGSOC (case T7) and one with LGSOC (case T15), we generated organoids at different time intervals and used variance analysis to identify the most variable genes across TDOs from each patient. The HGSOC patient presented 82 genes, while the LGSOC patient presented 113 genes (variance $\geq$ 5) (Tables S2 and S3). In both SOC patients, *MEG3* (maternally expressed 3) was the lncRNA exhibiting the highest variance throughout the disease course, and its expression levels decreased over time, which was confirmed by RT-qPCR (Fig. 2B). The differential expression analysis of the internal dataset revealed reduced *MEG3* expression levels in TDOs compared to normal tissue samples (Fig. 2C).

3.3. External data support lncRNA downregulation in SOC and suggest an interplay with the epigenetic machinery

To cross-validate our findings from SOC-derived organoids, we analyzed external RNA-Seq data from public repositories and SOC-derived organoids generated in another study [31]. The differential expression analysis comparing SOC samples from TCGA-OV (N = 337) with healthy ovarian tissue samples from GTEx (N = 180) detected 11, 143 DEGs, of which 5812 showed increased expression and 5331 exhibited decreased expression in tumors. Among the DEGs, 2057 were lncRNA genes (Fig. 3A), and 7460 were PCGs. A comparison with the internal dataset revealed 581 lncRNAs (20 %) differentially expressed in both cohorts (Fig. 2D). Most of these lncRNA genes (N = 373) showed decreased expression, while 148 exhibited augmented expression in SOC samples and TDOs. In parallel, 3490 PCGs (37.9 %) were differentially expressed in both cohorts, of which 3404 showed concordant expression profiles (1846 increased and 1558 decreased expression levels in SOC samples and TDOs).

The differential expression analysis using the TDOs dataset from Chen *et al.* [31] and our normal samples revealed 4653 DEGs: 1727 were overexpressed, and 2926 were down-expressed in TDOs. In this set of genes, 912 encoded lncRNAs (Fig. 3B) and 3262 encoded proteins. Moreover, 587 lncRNA genes (33.5 %) (Fig. 2E) and 3131 PCGs (58.3 %) were differentially expressed in both studies. Similarly to the TCGA/GTEx dataset, most DEGs encoding lncRNAs exhibited reduced levels (N = 450), while 134 showed increased levels in the external and internal TDOs. Considering the differentially expressed PCGs, 1604 were down-expressed, and 1527 were overexpressed in TDOs from both studies. Consistent with the results from our TDOs, lncRNA *MEG3* showed reduced expression in SOC tissue samples from TCGA and external TDOs (Fig. 3C).

We obtained a list of epigenetic regulators from the EpiFactors database to compare with the set of DEGs detected in our internal dataset. The lists of differentially expressed lncRNAs and PCGs associated with epigenetic regulation were included in Tables S4 and S5, respectively. According to EpiFactors, seven down-expressed lncRNAs (*MEG3*, *JPX*, *TARID*, *XIST*, *LINC00702*, *MAGI2-AS3*, and *HAND2-AS1*) and five overexpressed lncRNAs (*LINC00511*, *GNAS-AS1*, *LASTR*, *NEAT1*, and *HELLPAR*) were involved in the epigenetic regulation. Moreover, 68 PCGs with reduced expression and 100 PCGs with increased expression were involved in epigenetic processes. The overexpressed PCGs included several acknowledged components of the epigenetic machinery, such as DNA methyltransferases (*DNMT1* and *DNMT3B*), histone methyltransferase *EZH2* (enhancer of zeste 2 polycomb repressive complex 2 subunit), histone deacetylases (*HDAC7* and *HDAC9*), and histone demethylases (*KDM1B* and *KDM2A*). The enhanced expression of *DNMT3B*, *EZH2*, and *HDAC9* in SOC was validated in two independent transcriptomic datasets, as their overexpression was also observed in TCGA-OV samples and external TDOs compared to GTEx samples and our normal ovarian tissues, respectively (Fig. 4). Next, we utilized the lncPro method, embedded in the ncFANs database, to predict interactions between lncRNAs and proteins involved in epigenetic regulation, and constructed a network based on these results. *MEG3* was the lncRNA with the highest centrality in the generated network, and it was predicted to directly interact with 20 different epigenetic effectors, including EZH2 and DMT3B (Fig. 5A). We further investigated the relationship between *MEG3* and these effectors through their expression levels in SOC samples from TCGA-OV (N = 337). *MEG3* showed a negative correlation with *EZH2*, *EXOSC4*, *CBX3*, *MAZ*, *HDGF*, *CDK2*, and *PSIP1*, and a positive correlation with *DNMT3B*, *MYBBP1A*, *FBRSL1*, *SNAI2*, *TDRD3*, and *SMARCE1* (Fig. S3). These findings support the *MEG3* function as a hub of epigenetic regulation; therefore, its reduced levels in SOC potentially interfere with the modulation of downstream target genes, including those involved in cancer progression and therapy response.

The list of DEGs detected in our TDOs underwent gene set enrichment analysis, which resulted in 37 terms from the WikiPathways and 16 terms from the Kyoto Encyclopedia of Genes and Genomes (KEGG) database that were significantly enriched (Fig. 5B). The top pathways associated with overexpressed genes in TDOs included cell cycle, p53 signaling, bladder cancer, and the *RB* gene in cancer. Also, down-regulated genes were associated with Ras signaling, neovascularization processes, and cGMP-PKG signaling pathways.

3.4. Carboplatin response in OC cell lines and SOC-derived organoids after treatment with epi-drugs

Based on the overexpression of epigenetic effectors in our TDOs, we investigated if their inhibition could modulate the response to chemotherapeutic drugs in OC cell lines and SOC-derived TDOs by promoting the re-expression of epigenetically silenced genes. To this end, we selected doses of epi-drugs that maximized epigenetic reprogramming without producing cytotoxic effects, since we intended to perform a pretreatment followed by the challenge with carboplatin. The cell lines we subjected to drug testing, OVCAR8 and Ovc316, were chosen based on RNA-Seq data from our previous study [38]. Both cell lines exhibited the lowest *MEG3* expression levels among the carboplatin-resistant OC cell lines and subpopulations we had previously characterized (Fig. S4).

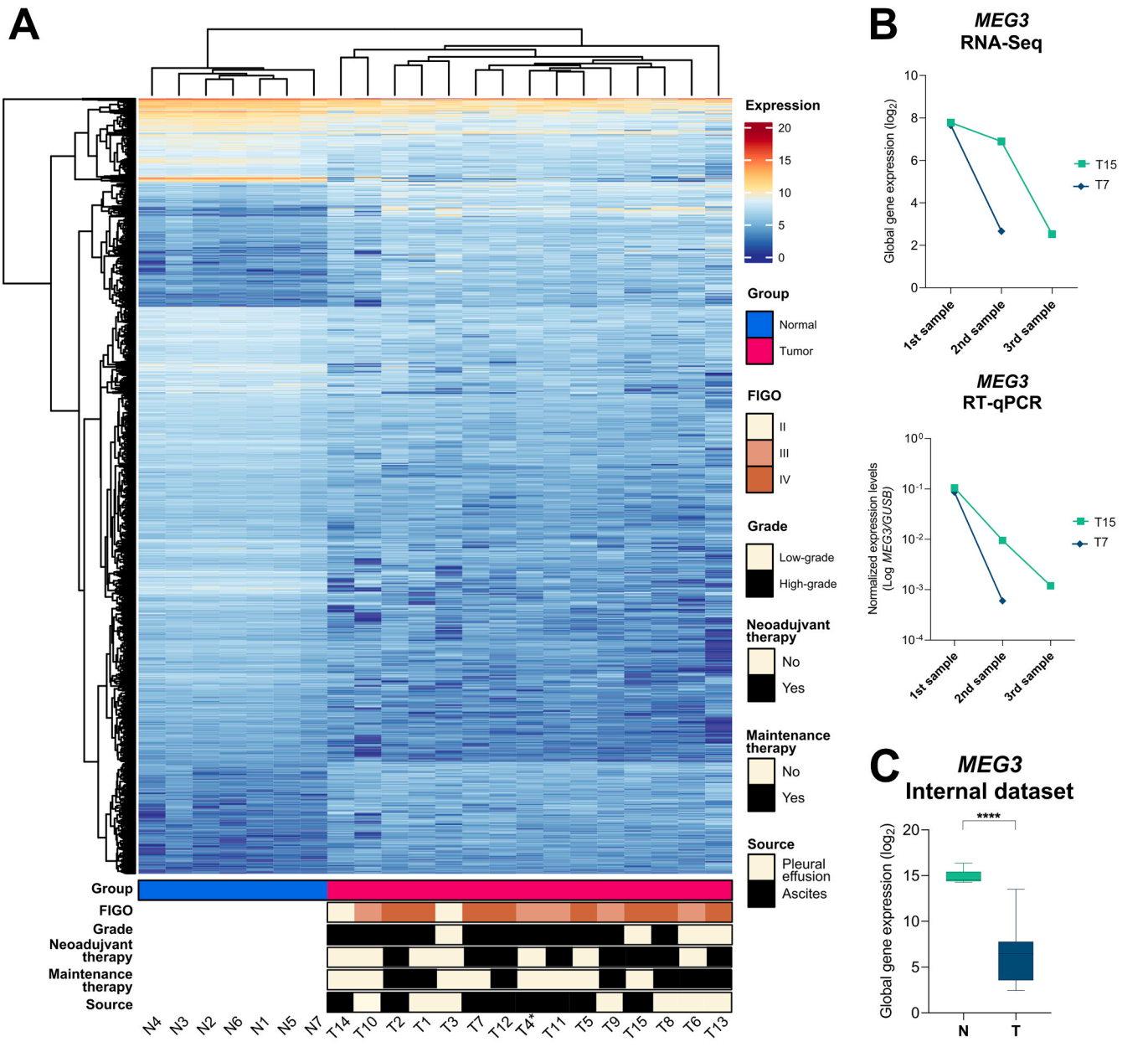

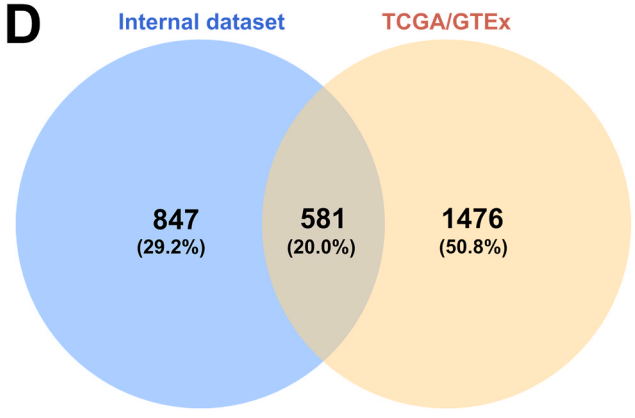

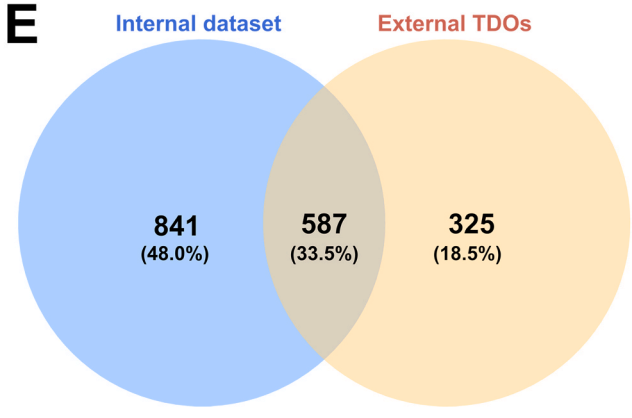

(caption on next page)

Fig. 2. Expression profile of the differentially expressed long noncoding RNAs (lncRNAs) identified in serous ovarian carcinomas. (A) The heatmap depicts lncRNAs differentially expressed in tumor-derived organoids (TDOs) compared with normal ovarian tissue samples from our cohort. Hierarchical clustering was performed assuming Euclidean distance. Columns and rows represent samples and genes, respectively. Red and blue indicate increased and decreased expression, respectively. The bottom bars show additional variables for each sample: group (normal or tumor), International Federation of Gynecology and Obstetrics (FIGO) stage (II, III or IV), histological grade (high- or low-grade), treatment information (neoadjuvant and/or maintenance therapy), and sample source (ascites or pleural effusion). *T4 was diagnosed with high-grade serous ovarian carcinoma with sarcoma component (carcinosarcoma). (B) The long noncoding RNA *MEG3* expression decreased over time, as detected by RNA-Seq and confirmed by RT-qPCR, in tumor-derived organoids from patients sampled multiple times. (C) The boxplot depicts the expression levels of the lncRNA *MEG3*, analyzed by RNA-Seq, in the internal cohort. The statistical difference was determined with the Mann–Whitney test. The Venn diagrams show the overlap of differentially expressed lncRNAs between the internal dataset and (D) the TCGA/GTEx samples or (E) the external TDOs [31]. ****$p < 0.0001$.

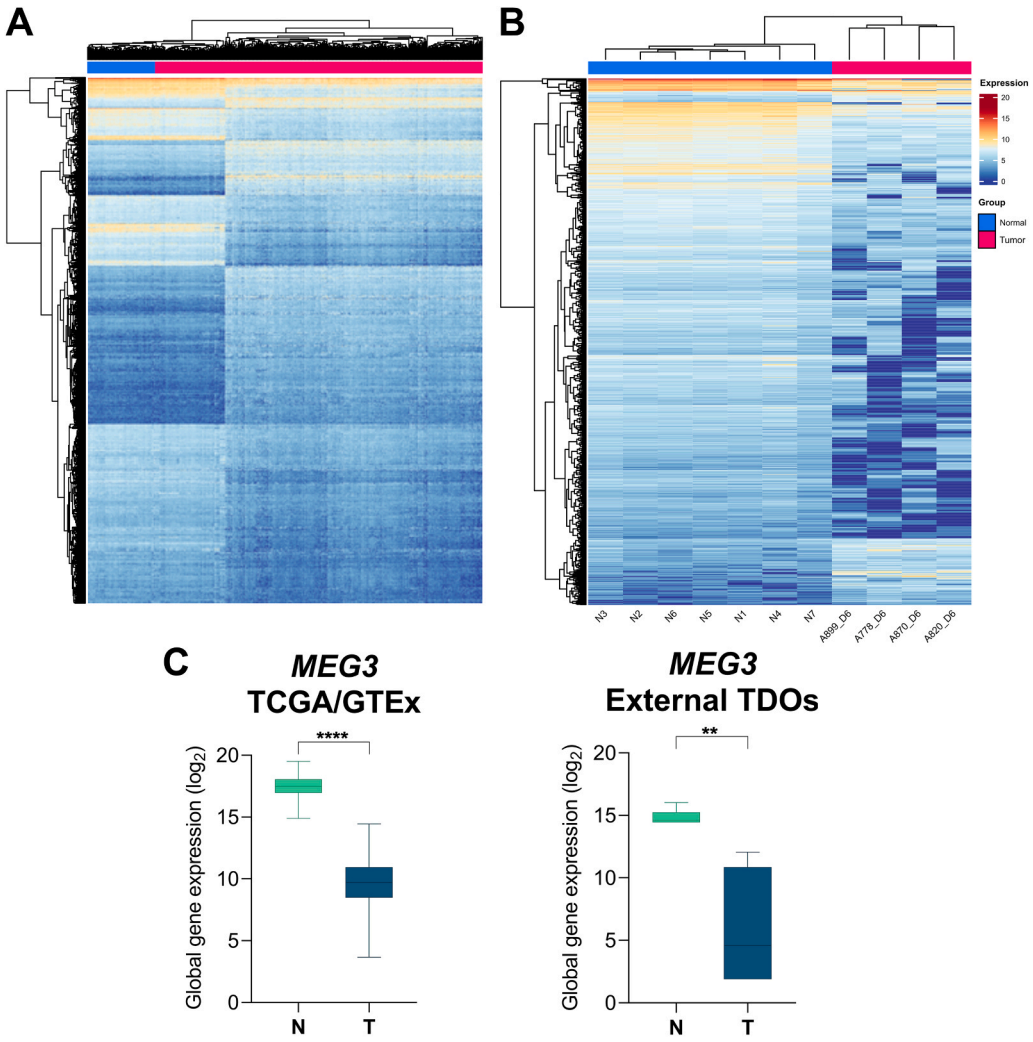

Fig. 3. Expression profile of the differentially expressed long noncoding RNAs (lncRNAs) identified in the external datasets. The heatmaps depict long noncoding RNAs differentially expressed in (A) SOC samples from The Cancer Genome Atlas compared with healthy ovarian samples from the Genotype-Tissue Expression Portal and in (B) external TDOs [31] compared to normal ovarian tissue samples from our cohort. Hierarchical clustering was performed assuming Euclidean distance. Columns and rows represent samples and genes, respectively. Red and blue indicate increased and decreased expression, respectively. The top bars identify tumor and normal samples. (C) The boxplots depict the expression levels of the lncRNA *MEG3*, analyzed by RNA-Seq, in the TCGA/GTEx samples and the external TDOs compared with our normal ovarian samples. The statistical difference was determined with the Mann–Whitney test. **$p < 0.01$; ****$p < 0.0001$.

Regarding the epigenetic effectors, OVCAR8 and Ovc316 exhibited the highest *DNMT1* and *EZH2* expression levels among the resistant OC cell lines, while *DNMT3A* and *DNMT3B* levels were intermediate (Fig. S4). Mass-spectrometry based proteomic data available from The Human Protein Atlas (https://www.proteinatlas.org/) showed that DNMT1, DNMT3B, and EZH2 proteins were detected in OVCAR8 cells, which exhibited one of the highest levels of EZH2 and DNMT1 expression among 58 other OC cell lines [41]. This information suggested that the selected cell lines were suitable for treatment with DNA methyltransferase inhibitor DAC and EZH2 inhibitor TAZ.

After exposing OC cells to DAC and TAZ, isolated or in combination, for 72 h, we determined that OVCAR8 and Ovc316 IC_{50} values were 6.006 μM and 1.545 μM for DAC, 12.17 μM and 7.42 μM for TAZ, and 5.776 μM and 6.411 μM for the combined epi-drugs, respectively. We selected DAC 1 μM and TAZ 2.5 μM, respectively, as the higher doses that did not affect cell viability (Fig. S5A and B). Low doses of DAC and TAZ were used based on previous preclinical studies that indicated that low doses of epi-drugs impair the self-renewal ability of cancer stem cells by enhancing the expression of genes that suppress malignancy, while causing less toxicity [42]. We exposed the cell lines OVCAR8 and Ovc316 to carboplatin at 50 and 100 μM, as we previously described [38].

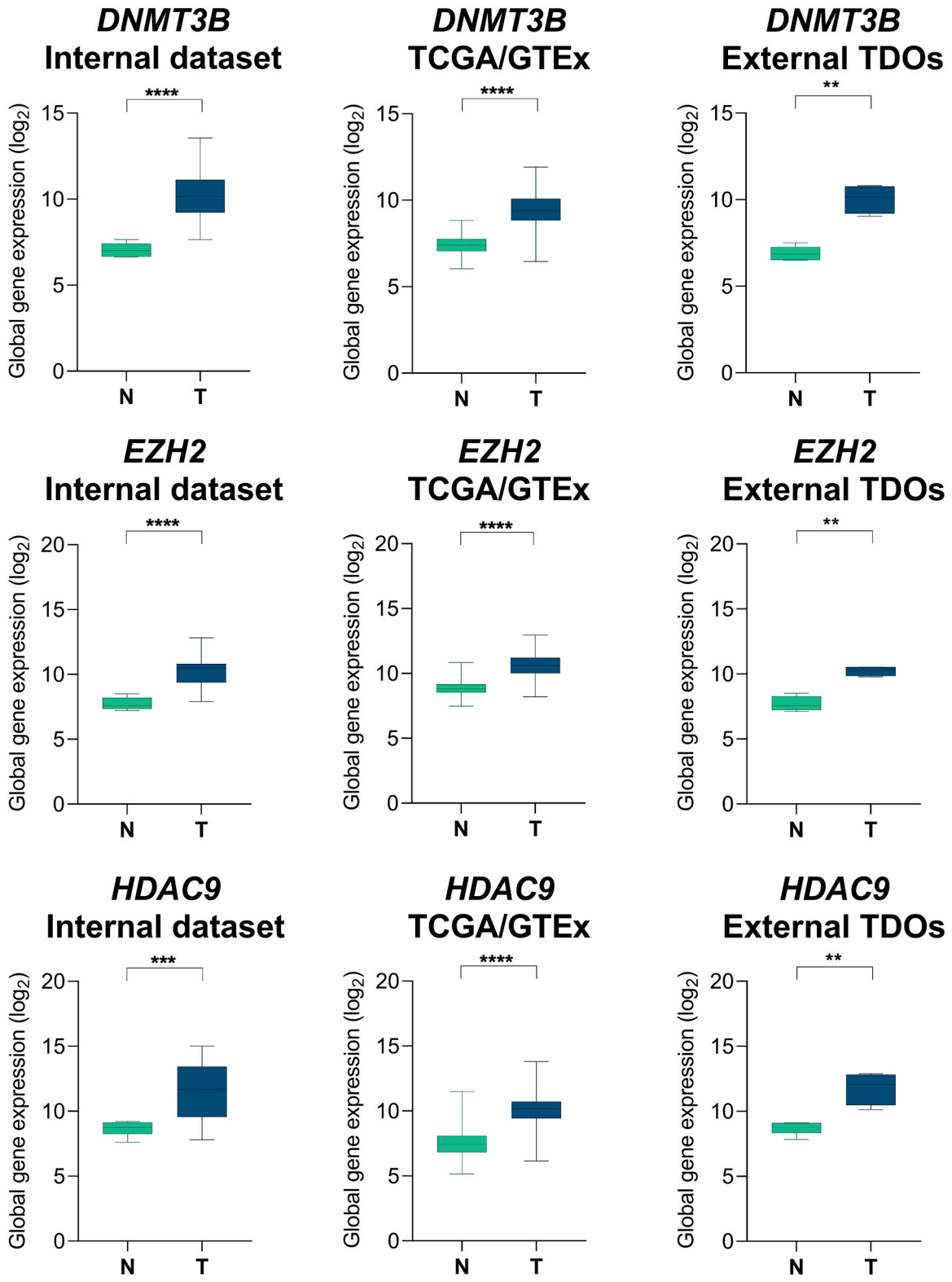

Fig. 4. Components of the epigenetic machinery overexpressed in serous ovarian carcinoma. The boxplots depict the expression levels of the protein-coding genes *DNMT3B*, *EZH2* and *HDAC9*, analyzed by RNA-Seq, from left to right, in the internal cohort, TCGA/ GTEx samples, and external TDOs compared with our normal ovarian samples. The statistical difference was determined with the Mann–Whitney test.

We also investigated the effects of pretreatment with epi-drugs DAC and TAZ on the viability of OVCAR8 and Ovc316 cell lines. DAC administered alone or in combination with TAZ promoted the re-sensitization to carboplatin at 50 and 100 μM in both cell lines (Fig. 6A). The TDO OV20231201PE exhibited increased sensitivity to carboplatin after pretreatment with DAC alone or in combination with TAZ, although the contribution of TAZ to this effect seems to be minor in TDOs and cell lines (Fig. 6B).

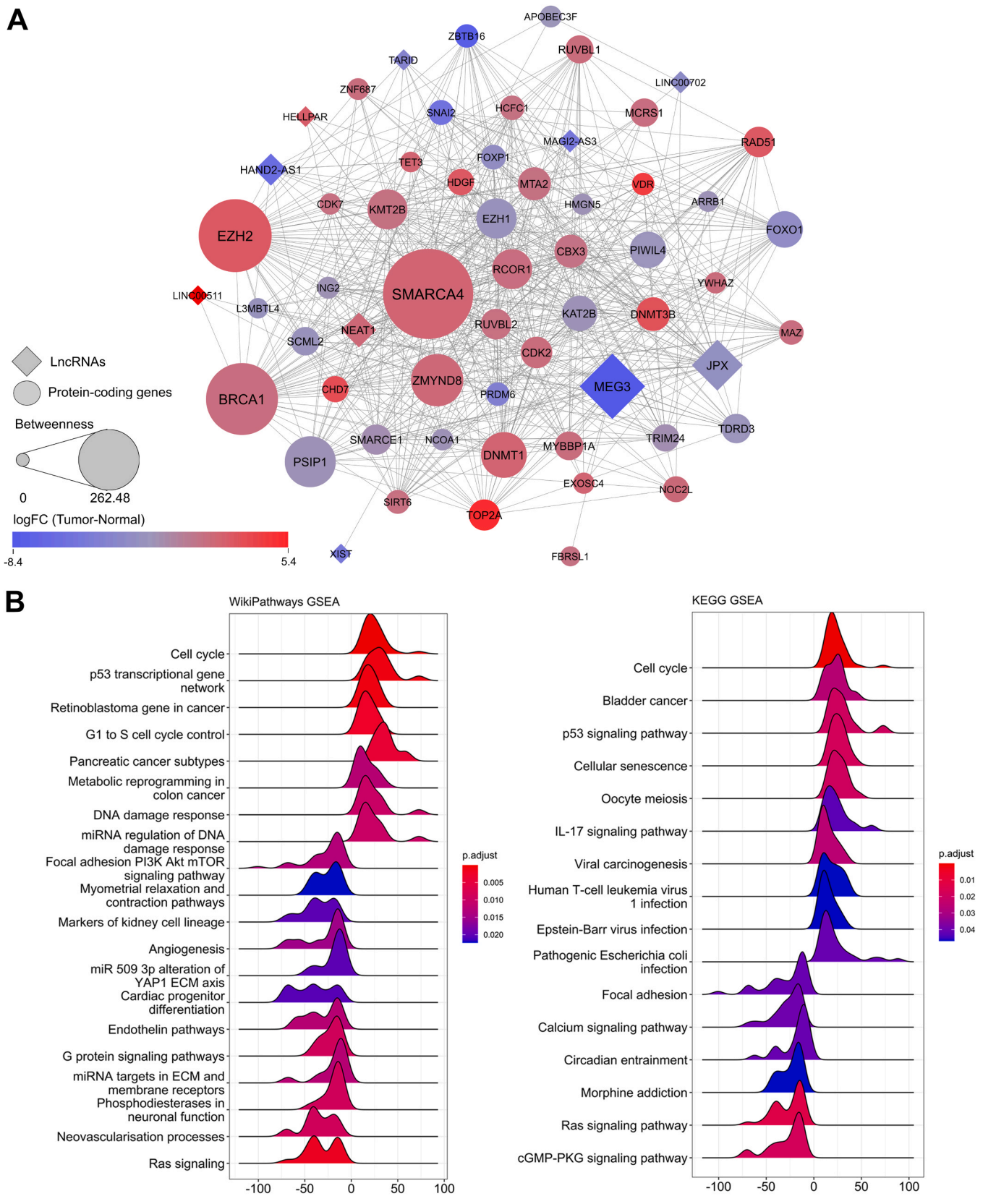

Fig. 5. Prediction of interactions between epigenetic regulators and identification of altered pathways in tumor-derived organoids (TDOs). (A) Interaction network of long noncoding RNAs (ncRNA) and protein-coding genes differentially expressed in TDOs and associated with epigenetic regulation. Larger circles indicate a higher betweenness centrality value of the node. Red and blue intensities represent gene expression fold-change (logFC). Gray lines highlight the interactions predicted using the ncRNA Functional Annotation Server (ncFANs) database. (B) The ridge plots show the pathways most significantly enriched for the differentially expressed genes detected in our TDOs based on gene set enrichment analysis (GSEA).

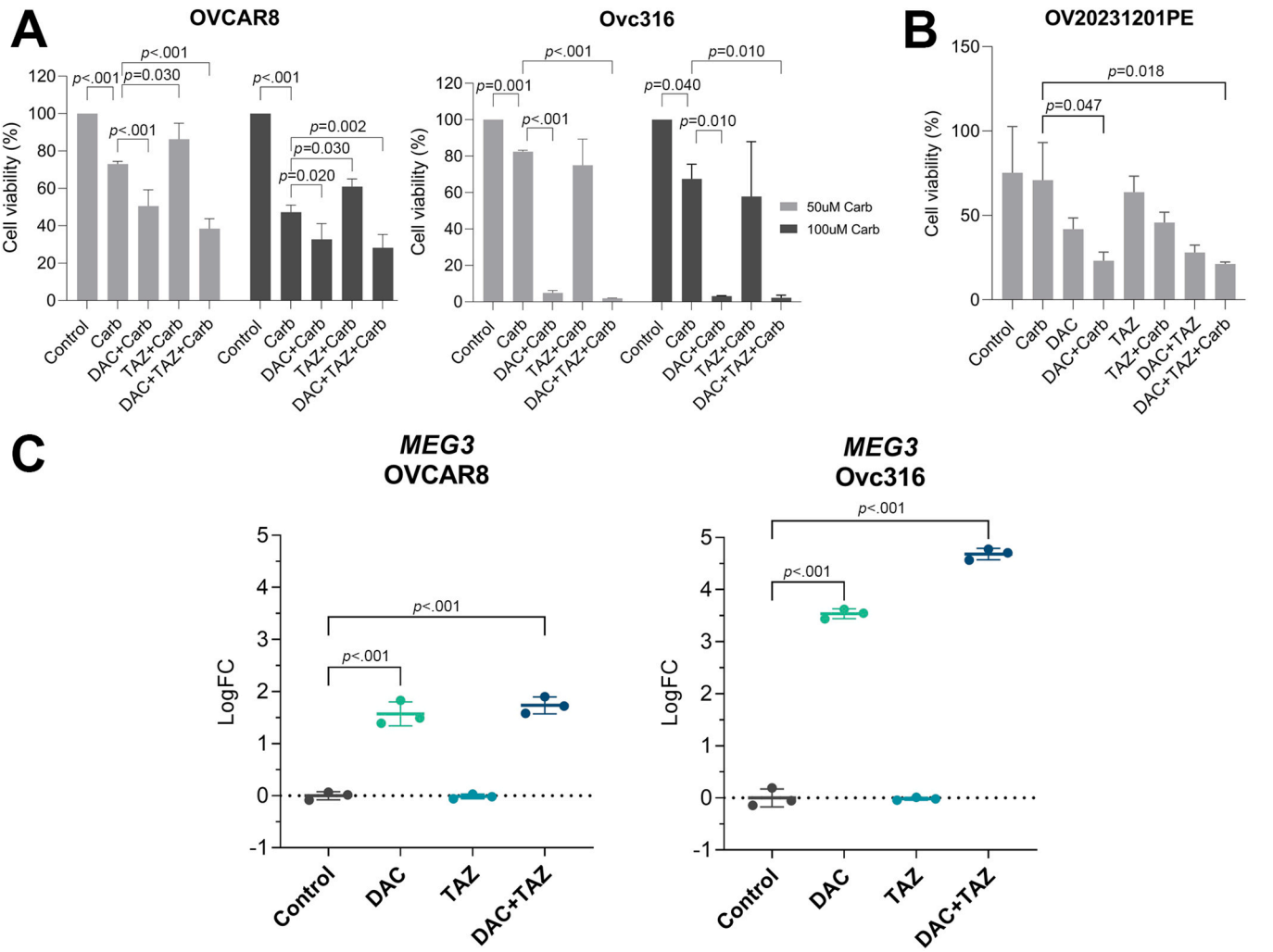

Fig. 6. Effects of epigenetic drugs on carboplatin sensitivity and *MEG3* expression in serous ovarian carcinoma (SOC). The bar plots represent the viability of (A) ovarian cancer cell lines OVCAR8 and Ovc316 and (B) SOC-derived organoids that were treated with decitabine (DAC) and tazemetostat (TAZ), isolated or in combination, before being challenged with carboplatin (Carb). All treatment conditions were performed in triplicate for both cell lines and organoids. The change in viability was calculated relative to the treatment with carboplatin alone. Statistical significance was evaluated by ordinary one-way ANOVA with Dunnett's multiple comparisons test (cell lines) or Kruskal-Wallis with Dunn's multiple comparisons test (TDO). (C) The dot plots show the *MEG3* expression levels, evaluated by RT-qPCR, in cell lines following the treatment with DAC and TAZ, alone or in combination. The gene expression fold-change (logFC) from the replicates is presented as the means ± standard deviations, represented by the center line and the error bars, respectively. Statistical significance was assessed by one-way ANOVA for all conditions compared to the control (DMSO). The *p*-values for the statistically significant differences ($p < 0.05$) are shown.

3.5. lncRNA MEG3 expression increased after epigenetic priming

The expression of the lncRNA *MEG3* was investigated by RT-qPCR to determine whether the epigenetic priming affected its levels. OVCAR8 and Ovc316 cell lines showed significantly higher *MEG3* expression after treatment with DAC isolated or combined with TAZ compared to the control (DMSO) (Fig. 6C).

4. Discussion

Tumor-derived organoid models have garnered increasing attention in basic and translational cancer research, as they are expected to reflect the inter- and intra-patient heterogeneity of human cancer, resembling the histopathological, genetic, and phenotypic aspects of the lesion of origin [43]. Moreover, TDOs allow for experimental manipulability while recapitulating the biological complexity, thereby filling a gap between conventional two-dimensional cell culture and animal models [13]. To date, several studies have generated OC organoids attaining an overall success rate of 30–90 % and a success rate of 58.3 % to nearly 100 % for organoids derived exclusively from ascites or pleural effusions [22,44]. The variability in success rates is expected, given the current lack of standardized medium formulations and procedures for establishing and maintaining OC organoids [44].

We established TDOs from malignant effusions for 15 out of 21 SOC patients, achieving a 71.4 % success rate, and expanded the cohort compared to other studies, which included up to 12 OC patients for organoid derivation using malignant fluids [22,31,45–47]. Also, the morphology of our TDOs varied significantly among our patients, as expected for SOC-derived organoids [48]. As a result, we established a TDO repertoire that captured SOC heterogeneity and investigated abnormally expressed genes, especially lncRNAs, that play a key role in expression modulation and consequently impact several biological processes.

Although there are ubiquitously expressed lncRNAs, these transcripts often exhibit higher spatial and temporal specificity than mRNAs, which is consistent with their role in determining cell state and differentiation programs under both physiological and pathophysiological conditions, such as cancer [8]. Herein, 1428 lncRNA were differentially expressed, mostly down-expressed in TDOs. No comparison was made between the transcriptional profiles and the previous treatment regimens, as our

cohort is heterogeneous in terms of treatment. Additionally, the sample size limits the statistical power to detect significant differences. However, previous studies have shown that chemotherapy influences the transcriptome profile of organoids, recapitulating therapy-induced changes and resistance mechanisms [49,50], which supports the use of organoids for studying disease progression and tailoring patient-specific treatment approaches.

To cross-validate the differential expression analysis results, we compared our findings with a set of SOCs and normal ovarian samples from TCGA/GTEx and four TDOs generated by Chen *et al.* [31]. Among the 983 lncRNAs exhibiting reduced expression in our TDOs, 373 and 450 were down-expressed in SOC samples from TCGA and external TDOs, respectively. In our cohort, lncRNA expression levels were also evaluated throughout the disease course for two patients with multiple samples collected, and we verified that *MEG3* was the lncRNA with the highest variance across TDOs in both patients. Notably, *MEG3* expression decreased over time, while both patients experienced progressive disease and ultimately died from the disease. Recently, Wegmann *et al.* demonstrated that integrating transcriptional and functional data of consecutive malignant effusion samples can uncover clinically actionable molecular alterations that occur after treatment [51]. This approach led to the detection of the overexpression of a druggable proto-oncogene at the time of relapse, which guided the therapeutic decision for one patient with lung adenocarcinoma. In our study, the analysis of external datasets confirmed decreased *MEG3* expression in SOC samples and TDOs. Accordingly, Sheng *et al.* showed that *MEG3* expression was lost in 70 % of OC tissue samples, primarily due to abnormal promoter hypermethylation [52]. Additionally, Braga *et al.* found a correlation between higher methylation levels of *MEG3* in primary OC tumor samples with advanced clinical stages, increased tumor size or extent, and metastasis [53]. Recently, *MEG3* downregulation was confirmed in HGSOC tissue samples [54]. Evidence from different OC subtypes revealed that induction of *MEG3* overexpression resulted in suppression of ovarian tumor cell growth, while *MEG3* knockdown led to increased cell proliferation and decreased cell apoptosis rate in OC cell lines [55]. Experiments using xenograft models demonstrated that *MEG3* knockdown resulted in larger ovarian tumor volumes and accelerated tumor growth rates [55]. Some of the known *MEG3* molecular mechanisms include sponging microRNAs, such as miR-885–5p, miR-376a, and miR-30e-3p, thereby upregulating the expression of *VASH1*, *RASA1*, and *LAMA4*, respectively, and hindering the OC malignant phenotype [55–57]. Lower levels of *MEG3* were correlated with advanced FIGO stages and reduced overall survival in OC patients [58,59]. Altogether, these findings suggest that reduced *MEG3* expression is associated with SOC progression and that epigenetic silencing is likely responsible for this lncRNA downregulation.

The expression of the imprinted gene *MEG3* was usually lost or reduced in a wide variety of human cancers [60,61]. The locus encoding this lncRNA contains several maternally and paternally expressed genes and is controlled by two differentially methylated regions (DMRs): the intergenic DMR, upstream from the *MEG3* gene, and the *MEG3*-DMR, which overlaps with the *MEG3* promoter [60]. *MEG3* was acknowledged as a tumor suppressor due to its pro-apoptotic and anti-proliferative activities *in vitro* and *in vivo* [60,61]. To exert these functions, nuclear retained lncRNAs, such as *MEG3,* can recruit or sequester proteins that affect transcription through epigenetic regulatory processes, including DNA methylation, chromatin remodeling, and histone marks deposition [62,63]. Among the DEGs identified in our TDOs, we detected 180 previously characterized as epigenetic regulators, encompassing *MEG3* and 11 additional lncRNAs, and 168 PCGs. Experimental evidence showed that *MEG3* binds to EZH2 in prostate, breast, gallbladder, pancreatic, and lung cancer cells with consequences for cell proliferation, migration, and invasion [61,62,64]. EZH2 is a repressive histone modifier, part of polycomb repressive complex 2 (PRC2), which catalyzes H3K27 methylation, promoting gene silencing and is often upregulated in cancer, especially in advanced stages [65]. Using a computational approach [35] to explore the interactions between the epigenetic regulators abnormally expressed in our TDOs, *MEG3* was predicted to interact with 20 protein regulators, including EZH2 and DNA methyltransferase 3 beta (DNMT3B). Also, *MEG3* expression levels were correlated with *EZH2* and *DNMT3B* in SOC samples from TCGA-OV. DNMT3B contributes to establishing *de novo* DNA methylation profiles at previously unmethylated loci, is crucial during embryonic development, and usually presents augmented expression in human cancers [66]. In accordance with prior reports, we observed that genes *EZH2* and *DNMT3B* were overexpressed in the internal and external TDOs and SOC tissue samples. Therefore, we propose that *MEG3* is a hub for fine-tuning gene expression through epigenetic mechanisms, and its downregulation prevents this lncRNA from playing tumor-suppressive roles that could control SOC aggressive behavior. This mechanism has yet to be fully demonstrated in SOC, although *MEG3* interaction with EZH2 has been characterized in other tumor types.

Zhang *et al.* detected increased *MEG3* expression and lessened resistance to cisplatin after treating platinum-resistant OC cells with curcumin [67]. Curcumin served as a demethylating agent, reversing *MEG3* promoter hypermethylation and restoring the lncRNA expression. Herein, OC cell lines characterized as carboplatin-resistant [38] were treated with two FDA-approved epi-drugs, one broad- and one narrow-spectrum epigenetic reprogrammer, DAC and TAZ, respectively. DAC promotes genome-wide changes in gene expression, functioning as a cytidine analog that is incorporated into DNA by DNA methyltransferases (DNMTs), while TAZ specifically inhibits the enzymatic activity of EZH2 [68,69]. Subsequently, we assessed the expression of *MEG3* and the sensitivity of OC cells to carboplatin. OVCAR8 and Ovc316 cell lines showed significantly higher *MEG3* expression after the treatment with DAC alone or in combination with TAZ. Additionally, both cell lines exhibited enhanced sensitivity to carboplatin following pretreatment with DAC, isolated or combined with TAZ, whereas no significant effect was observed after the administration of TAZ individually. Most approved drugs targeting epigenetic regulators are applied to treat hematologic malignancies, since studies on their therapeutic potential in solid tumors are limited. However, recent clinical trials showed that selected groups of platinum-resistant OC patients benefited from epigenetic priming with DNMT inhibitors [70,71]. On the other hand, clinical trials that administered EZH2 inhibitors alone did not show effective antitumor activity in solid tumors with augmented *EZH2* expression, including ovarian cancer [69]. Despite *EZH2* expression being associated with cell proliferation and invasion, apoptosis inhibition, and enhanced angiogenesis in epithelial OC, the efficacy of the different classes of drugs targeting EZH2 depends on the mechanisms by which EZH2 contributes to tumorigenesis [72,73]. Chen *et al.* reported that EZH2 also plays a noncanonical role as a transcriptional activator in OVCAR8 cells apart from its PRC2-dependent histone methyltransferase activity [73]. In the same study, two inhibitors inducing EZH2 degradation exhibited greater anticancer efficacy in OC cell lines and xenografts compared to the other two inhibitors targeting its methyltransferase activity, including TAZ. This may help explain the limited effect that we observed after pre-treatment with TAZ.

One TDO derived from malignant effusions also received the same treatment regimen administered to the cell lines. We found an increased sensitivity to carboplatin after pretreatment with DAC alone or in combination with TAZ. To the best of our knowledge, ours is the first study to test this treatment regimen in organoids derived from OC patients. Recently, Gerton *et al.* combined DNMT inhibitor 5-azacytidine and HDAC inhibitor givinostat with immune checkpoint blockade to treat spheroids derived from ascites of HGSOC patients [19]. Their findings suggested that the use of epi-drugs could potentiate the immunotherapy response.

While our study offers novel insights into the applicability of organoids derived from malignant effusions as preclinical models, we must acknowledge certain limitations. First, we derived organoids from 21 SOC patients; however, TDOs presented low proliferation rates in six

cases and were therefore excluded. This may be explained by the lack of certain growth-promoting supplements in the culture medium, such as FGF-4 [22]. Second, primary tumor tissues from SOC patients in our cohort were not available for RNA-Seq analysis; however, we consistently observed the abnormal expression of the genes of interest in our TDOs, TCGA-OV primary tumors (N = 337), and external TDOs (N = 4) compared to normal samples. Third, an assay for modulating *MEG3* expression, such as CRISPR activation, would be relevant to determine whether the increased cytotoxic effects of carboplatin we observed in OC cells and SOC-derived organoids are due to *MEG3* enhanced levels. Lastly, the pre-treatment with epi-drugs followed by carboplatin was investigated in one case with TDOs for successive tests. Most TDOs were cryopreserved, which impaired their viability upon resuscitation and could affect the treatment regimen assessment. The selected TDO was exposed to treatment right after culture establishment without a cryopreservation step. Expanding the number of SOC-derived organoids exposed to our treatment approach could strengthen the evidence for the efficacy of epi-drugs in restoring platinum sensitivity.

Although incipient, the use of TDOs to select individualized cancer treatment seems promising and has been reported by two prospective clinical trials with colorectal cancer patients [74,75], while several ongoing trials are set out to establish organoid-guided protocols to treat diverse tumor types, including pancreatic, ovarian, gastric, and breast cancer (ClinicalTrials.gov IDs: NCT04931394, NCT05813509, NCT05842187, NCT06102824). Recently, the first case employing ascites-derived organoids for drug sensitivity screening of a patient with recurrent HGSOC was reported [76]. These and additional prospective studies are essential for confirming the reliability of TDOs in identifying new clinically actionable targets and testing patient-specific therapeutic approaches for HGSOC, thereby helping to translate basic research findings into patient treatment.

5. Conclusions

We developed organoids from malignant effusions of SOC patients and achieved a high success rate. RNA-Seq analyses were performed in our set of TDOs, revealing the altered expression of several lncRNAs and protein-coding genes, including epigenetic regulators. We focused on the interplay between epigenetic regulators since they are responsible for fine-tuning cellular transcriptional programs and influencing the behavior of SOCs. We demonstrated that the lncRNA *MEG3* is downregulated in SOC across different specimens (tissues, TDOs, and cell lines) and independent datasets, and that its expression, along with carboplatin sensitivity, was enhanced following treatment of OC cells with FDA-approved epigenetic drugs. Therefore, our findings suggest that *MEG3* may play a significant role in epigenetic regulation and therapy response in serous ovarian cancer.

Abbreviations

3D three-dimensional
DAC decitabine
DEGs differentially expressed genes
DMEM Dulbecco's modified Eagle medium
DMRs differentially methylated regions
DNMTs DNA methyltransferases
FC fold-change
FDR false discovery rate
FGF fibroblast growth factor
FIGO International Federation of Gynaecology and Obstetrics
GRCh38 Genome Reference Consortium Human Build 38
GSEA gene set enrichment analysis
GTEx Genotype-Tissue Expression Portal
HGSOC high-grade serous ovarian carcinoma
KEGG Kyoto Encyclopedia of Genes and Genomes
LGSOC low-grade serous ovarian carcinoma
LncRNAs long noncoding RNAs
ncFANs ncRNA Functional Annotation Server
OC ovarian cancer
PCGs protein-coding genes
PRC2 polycomb repressive complex 2
RNA-Seq RNA sequencing
SOC serous ovarian carcinoma
STAR Spliced Transcripts Alignment to a Reference
TAZ tazemetostat
TCGA The Cancer Genome Atlas
TDOs tumor-derived organoids

CRediT authorship contribution statement

Luiza Côrtes: Writing – review & editing, Visualization, Investigation, Formal analysis. **Debora Kazumi Maeda:** Writing – review & editing, Visualization, Investigation, Formal analysis. **Daniela Bizinelli:** Writing – review & editing, Visualization, Formal analysis. **Rolando André Rios Villacis:** Writing – review & editing, Visualization, Investigation. **Claudia Aparecida Rainho:** Writing – review & editing, Visualization, Supervision, Methodology. **Silvia Regina Rogatto:** Writing – review & editing, Writing – original draft, Visualization, Supervision, Project administration, Methodology, Funding acquisition, Conceptualization. **Naiade Calanca:** Writing – review & editing, Writing – original draft, Visualization, Investigation, Formal analysis. **Lars Henrik Jensen:** Writing – review & editing, Visualization, Project administration, Methodology, Funding acquisition. **Mads Malik Aagaard:** Writing – review & editing, Visualization, Formal analysis. **Hellen Kuasne:** Writing – review & editing, Visualization, Formal analysis. **Karina Dahl Steffensen:** Writing – review & editing, Visualization, Methodology. **Lars Ulrik Fokdal:** Writing – review & editing, Visualization, Formal analysis.

Informed consent statement

Informed consent was obtained from all subjects involved in the study.

Institutional review board statement

The study was conducted in accordance with the Declaration of Helsinki and approved by the Ethics Committee of the Region of Southern Denmark (S-20190102) and the Danish Data Protection Agency (Case No. 19/37168).

Funding sources

This research was supported by the Region of Southern Denmark Research Fund (J.nr.: 20/14277). N.C. and D.K.M. were granted scholarships from the Brazilian Federal Agency for Support and Evaluation of Graduate Education (CAPES) within the scope of the CAPES-PrInt Program (process number 88887.310463/2018–00, mobility numbers 88887.570391/2020–00 and 88887.889772/2023–00).

Declaration of Competing Interest

The authors declare that they have no known competing financial interests or personal relationships that could have appeared to influence the work reported in this paper.

Acknowledgments

Study data were collected and managed using REDCap electronic data capture tools hosted by OPEN (OP_1001), Open Patient Data Explorative Network, Odense University Hospital, University of Southern Denmark, DK. The authors are grateful to the patients who agreed to

participate in this study. We thank Monica Søgaard Tronhjem for her help in sample collection and Luisa Matos do Canto for her technical assistance.

Appendix A. Supporting information

Supplementary data associated with this article can be found in the online version at doi:10.1016/j.biopha.2025.118668.

Data Availability

Data will be made available on request.

References

[1] S.P. Blagden, Harnessing pandemonium: the clinical implications of tumor heterogeneity in ovarian cancer, Front. Oncol. 5 (2015), https://doi.org/10.3389/fonc.2015.00149.

[2] K. Gaitskell, C. Hermon, I. Barnes, K. Pirie, S. Floud, J. Green, V. Beral, G.K. Reeves, Ovarian cancer survival by stage, histotype, and pre-diagnostic lifestyle factors, in the prospective UK million women study, Cancer Epidemiol. 76 (2022), https://doi.org/10.1016/j.canep.2021.102074.

[3] M.A. Lisio, L. Fu, A. Goyeneche, Z.H. Gao, C. Telleria, High-grade serous ovarian cancer: basic sciences, clinical and therapeutic standpoints, Int. J. Mol. Sci. 20 (2019), https://doi.org/10.3390/ijms20040952.

[4] D.L. Richardson, R.N. Eskander, D.M. O'Malley, Advances in ovarian cancer care and unmet treatment needs for patients with platinum resistance, JAMA Oncol. 9 (2023) 851, https://doi.org/10.1001/jamaoncol.2023.0197.

[5] R.N. Grisham, B.L. Manning-Geist, M.H. Chui, The highs and lows of serous ovarian cancer, Cancer 129 (2023) 2613–2620, https://doi.org/10.1002/cncr.34903.

[6] Y. Xiao, M. Bi, H. Guo, M. Li, Multi-omics approaches for biomarker discovery in early ovarian cancer diagnosis, EBioMedicine 79 (2022) 104001, https://doi.org/10.1016/j.ebiom.2022.104001.

[7] S. Moufarrij, M. Dandapani, E. Arthofer, S. Gomez, A. Srivastava, M. Lopez-Acevedo, A. Villagra, K.B. Chiappinelli, Epigenetic therapy for ovarian cancer: promise and progress, Clin. Epigenet. 11 (2019), https://doi.org/10.1186/s13148-018-0602-0.

[8] J.S. Mattick, P.P. Amaral, P. Carninci, S. Carpenter, H.Y. Chang, L.L. Chen, R. Chen, C. Dean, M.E. Dinger, K.A. Fitzgerald, T.R. Gingeras, M. Guttman, T. Hirose, M. Huarte, R. Johnson, C. Kanduri, P. Kapranov, J.B. Lawrence, J.T. Lee, J. T. Mendell, T.R. Mercer, K.J. Moore, S. Nakagawa, J.L. Rinn, D.L. Spector, I. Ulitsky, Y. Wan, J.E. Wilusz, M. Wu, Long non-coding RNAs: definitions, functions, challenges and recommendations, Nat. Rev. Mol. Cell Biol. 24 (2023) 430–447, https://doi.org/10.1038/s41580-022-00566-8.

[9] C. Abildgaard, L.M. Do Canto, K.D. Steffensen, S.R. Rogatto, Long Non-coding RNAs involved in resistance to chemotherapy in ovarian cancer, Front. Oncol. 9 (2020) 1–17, https://doi.org/10.3389/fonc.2019.01549.

[10] Y. Lou, H. Jiang, Z. Cui, X. Wang, L. Wang, Y. Han, Gene microarray analysis of lncRNA and mRNA expression profiles in patients with high-grade ovarian serous cancer, Int. J. Mol. Med. 42 (2018) 91–104, https://doi.org/10.3892/ijmm.2018.3588.

[11] Q. Li, J. Zhang, J. Zhou, B. Yang, P. Liu, L. Cao, L. Jing, H. Liu, LncRNAs are novel biomarkers for differentiating between cisplatin-resistant and cisplatin-sensitive ovarian cancer, Oncol. Lett. 15 (2018) 8363–8370, https://doi.org/10.3892/ol.2018.8433.

[12] H. Clevers, Modeling development and disease with organoids, Cell 165 (2016) 1586–1597, https://doi.org/10.1016/j.cell.2016.05.082.

[13] M. Li, J.C. Izpisua Belmonte, Organoids — preclinical models of human disease, N. Engl. J. Med. 380 (2019) 569–579, https://doi.org/10.1056/nejmra1806175.

[14] C.E. Ford, B. Werner, N.F. Hacker, K. Warton, The untapped potential of ascites in ovarian cancer research and treatment, Br. J. Cancer 123 (2020) 9–16, https://doi.org/10.1038/s41416-020-0875-x.

[15] E. Kipps, D.S.P. Tan, S.B. Kaye, Meeting the challenge of ascites in ovarian cancer: new avenues for therapy and research, Nat. Rev. Cancer 13 (2013) 273–282, https://doi.org/10.1038/nrc3432.

[16] J.M. Porcel, A. Esquerda, M. Vives, S. Bielsa, Etiology of pleural effusions: analysis of more than 3,000 consecutive thoracenteses, Arch. Bronconeumol. Engl. Ed. 50 (2014) 161–165, https://doi.org/10.1016/j.arbr.2014.03.012.

[17] I. Matte, P. Garde-Granger, P. Bessette, A. Piché, Serum CA125 and ascites leptin level ratio predicts baseline clinical resistance to first-line platinum-based treatment and poor prognosis in patients with high grade serous ovarian cancer, Am. J. Cancer Res. 9 (2019) 160–170. ⟨http://www.ncbi.nlm.nih.gov/pubmed/30755819⟩.

[18] J.E. den Ouden, G.J.R. Zaman, J. Dylus, A.M. van Doornmalen, W.R. Mulder, Y. Grobben, W.E. van Riel, J.A. de Hullu, R.C. Buijsman, A.M. van Altena, Chemotherapy sensitivity testing on ovarian cancer cells isolated from malignant ascites, Oncotarget 11 (2020) 4570–4581, https://doi.org/10.18632/oncotarget.27827.

[19] T.J. Gerton, A. Green, M. Campisi, M. Chen, I. Gjeci, N. Mahadevan, C.A.A. Lee, R. Mishra, H.V. Vo, K. Haratani, Z.H. Li, K.T. Hasselblatt, B. Testino, T. Connor, C. G. Lian, K.M. Elias, P. Lizotte, E.V. Ivanova, D.A. Barbie, D.M. Dinulescu, Development of a Patient-Derived 3D Immuno-Oncology platform to potentiate immunotherapy responses in Ascites-Derived circulating tumor cells, Cancers 15 (2023), https://doi.org/10.3390/cancers15164128.

[20] R.F. Carvalho, L.M. do Canto, C. Abildgaard, M.M. Aagaard, M.S. Tronhjem, M. Waldstrøm, L.H. Jensen, K.D. Steffensen, S.R. Rogatto, Single-cell and bulk RNA sequencing reveal ligands and receptors associated with worse overall survival in serous ovarian cancer, Cell Commun. Signal. 20 (2022) 176, https://doi.org/10.1186/s12964-022-00991-4.

[21] O. Kopper, C.J. de Witte, K. Lõhmussaar, J.E. Valle-Inclan, N. Hami, L. Kester, A. V. Balgobind, J. Korving, N. Proost, H. Begthel, L.M. van Wijk, S.A. Revilla, R. Theeuwsen, M. van de Ven, M.J. van Roosmalen, B. Ponsioen, V.W.H. Ho, B. G. Neel, T. Bosse, K.N. Gaarenstroom, H. Vrieling, M.P.G. Vreeswijk, P.J. van Diest, P.O. Witteveen, T. Jonges, J.L. Bos, A. van Oudenaarden, R.P. Zweemer, H.J. G. Snippert, W.P. Kloosterman, H. Clevers, An organoid platform for ovarian cancer captures intra- and interpatient heterogeneity, Nat. Med 25 (2019) 838–849, https://doi.org/10.1038/s41591-019-0422-6.

[22] W. Senkowski, L. Gall-Mas, M.M. Falco, Y. Li, K. Lavikka, M.C. Kriegbaum, J. Oikkonen, D. Bulanova, E.J. Pietras, K. Voßgröne, Y.J. Chen, E.P. Erkan, J. Dai, A. Lundgren, M.K. Grønning Høg, I.M. Larsen, T. Lamminen, K. Kaipio, J. Huvila, A. Virtanen, L. Engelholm, P. Christiansen, E. Santoni-Rugiu, K. Huhtinen, O. Carpén, J. Hynninen, S. Hautaniemi, A. Vähärautio, K. Wennerberg, A platform for efficient establishment and drug-response profiling of high-grade serous ovarian cancer organoids, Dev. Cell 58 (2023) 1106–1121.e7, https://doi.org/10.1016/j.devcel.2023.04.012.

[23] P. Ewels, M. Magnusson, S. Lundin, M. Käller, MultiQC: summarize analysis results for multiple tools and samples in a single report, Bioinformatics 32 (2016) 3047–3048, https://doi.org/10.1093/bioinformatics/btw354.

[24] A. Dobin, C.A. Davis, F. Schlesinger, J. Drenkow, C. Zaleski, S. Jha, P. Batut, M. Chaisson, T.R. Gingeras, STAR: ultrafast universal RNA-seq aligner, Bioinformatics 29 (2013) 15–21, https://doi.org/10.1093/bioinformatics/bts635.

[25] Y. Liao, G.K. Smyth, W. Shi, Featurecounts: an efficient general purpose program for assigning sequence reads to genomic features, Bioinformatics 30 (2014) 923–930, https://doi.org/10.1093/bioinformatics/btt656.

[26] S. Durinck, P.T. Spellman, E. Birney, W. Huber, Mapping identifiers for the integration of genomic datasets with the R/Bioconductor package biomart, Nat. Protoc. 4 (2009) 1184–1191, https://doi.org/10.1038/nprot.2009.97.

[27] M.I. Love, W. Huber, S. Anders, Moderated estimation of fold change and dispersion for RNA-seq data with DESeq2, Genome Biol. 15 (2014) 550, https://doi.org/10.1186/s13059-014-0550-8.

[28] M.E. Ritchie, B. Phipson, D. Wu, Y. Hu, C.W. Law, W. Shi, G.K. Smyth, Limma powers differential expression analyses for RNA-sequencing and microarray studies, e47–e47, Nucleic Acids Res. 43 (2015), https://doi.org/10.1093/nar/gkv007.

[29] A. Colaprico, T.C. Silva, C. Olsen, L. Garofano, C. Cava, D. Garolini, T.S. Sabedot, T. M. Malta, S.M. Pagnotta, I. Castiglioni, M. Ceccarelli, G. Bontempi, H. Noushmehr, TCGAbiolinks: an R/Bioconductor package for integrative analysis of TCGA data, e71–e71, Nucleic Acids Res. 44 (2016), https://doi.org/10.1093/nar/gkv1507.

[30] M.J. Goldman, B. Craft, M. Hastie, K. Repečka, F. McDade, A. Kamath, A. Banerjee, Y. Luo, D. Rogers, A.N. Brooks, J. Zhu, D. Haussler, Visualizing and interpreting cancer genomics data via the xena platform, Nat. Biotechnol. 38 (2020) 675–678, https://doi.org/10.1038/s41587-020-0546-8.

[31] H. Chen, K. Gotimer, C. De Souza, C.G. Tepper, A.N. Karnezis, G.S. Leiserowitz, J. Chien, L.H. Smith, Short-term organoid culture for drug sensitivity testing of high-grade serous carcinoma, Gynecol. Oncol. 157 (2020) 783–792, https://doi.org/10.1016/j.ygyno.2020.03.026.

[32] J.T. Leek, W.E. Johnson, H.S. Parker, A.E. Jaffe, J.D. Storey, The sva package for removing batch effects and other unwanted variation in high-throughput experiments, Bioinformatics 28 (2012) 882–883, https://doi.org/10.1093/bioinformatics/bts034.

[33] D. Marakulina, I.E. Vorontsov, I.V. Kulakovskiy, A. Lennartsson, F. Drabløs, Y. A. Medvedeva, EpiFactors 2022: expansion and enhancement of a curated database of human epigenetic factors and complexes, Nucleic Acids Res 51 (2023) D564–D570, https://doi.org/10.1093/nar/gkac989.

[34] Y. Zhang, D. Bu, P. Huo, Z. Wang, H. Rong, Y. Li, J. Liu, M. Ye, Y. Wu, Z. Jiang, Q. Liao, Y. Zhao, ncFANs v2.0: an integrative platform for functional annotation of non-coding RNAs, Nucleic Acids Res 49 (2021) W459–W468, https://doi.org/10.1093/nar/gkab435.

[35] Q. Lu, S. Ren, M. Lu, Y. Zhang, D. Zhu, X. Zhang, T. Li, Computational prediction of associations between long non-coding RNAs and proteins, BMC Genom. 14 (2013), https://doi.org/10.1186/1471-2164-14-651.

[36] Y. Tang, M. Li, J. Wang, Y. Pan, F.X. Wu, CytoNCA: a cytoscape plugin for centrality analysis and evaluation of protein interaction networks, BioSystems 127 (2015) 67–72, https://doi.org/10.1016/j.biosystems.2014.11.005.

[37] N.T. Doncheva, Y. Assenov, F.S. Domingues, M. Albrecht, Topological analysis and interactive visualization of biological networks and protein structures, Nat. Protoc. 7 (2012) 670–685, https://doi.org/10.1038/nprot.2012.004.

[38] C. Abildgaard, L.M. do Canto, C.A. Rainho, F.A. Marchi, N. Calanca, M. Waldstrøm, K.D. Steffensen, S.R. Rogatto, The long Non-Coding RNA SNHG12 as a mediator of carboplatin resistance in ovarian cancer via epigenetic mechanisms, Cancers 14 (2022) 1664, https://doi.org/10.3390/cancers14071664.

[39] K.J. Livak, T.D. Schmittgen, Analysis of relative gene expression data using real-time quantitative PCR and the $2^{-\Delta\Delta CT}$ method, Methods 25 (2001) 402–408, https://doi.org/10.1006/meth.2001.1262.

[40] Z. Gu, R. Eils, M. Schlesner, Complex heatmaps reveal patterns and correlations in multidimensional genomic data, Bioinformatics 32 (2016) 2847–2849, https://doi.org/10.1093/bioinformatics/btw313.

[41] H. Jin, C. Zhang, M. Zwahlen, K. von Feilitzen, M. Karlsson, M. Shi, M. Yuan, X. Song, X. Li, H. Yang, H. Turkez, L. Fagerberg, M. Uhlén, A. Mardinoglu, Systematic transcriptional analysis of human cell lines for gene expression landscape and tumor representation, Nat. Commun. 14 (2023) 5417, https://doi.org/10.1038/s41467-023-41132-w.
[42] M. Karahoca, R.L. Momparler, Pharmacokinetic and pharmacodynamic analysis of 5-aza-2'-deoxycytidine (decitabine) in the design of its dose-schedule for cancer therapy, Clin. Epigenet. 5 (2013) 3, https://doi.org/10.1186/1868-7083-5-3.
[43] B.L. LeSavage, R.A. Suhar, N. Broguiere, M.P. Lutolf, S.C. Heilshorn, Next-generation cancer organoids, Nat. Mater. 21 (2022) 143–159, https://doi.org/10.1038/s41563-021-01057-5.
[44] T. Qin, J. Fan, F. Lu, L. Zhang, C. Liu, Q. Xiong, Y. Zhao, G. Chen, C. Sun, Harnessing preclinical models for the interrogation of ovarian cancer, J. Exp. Clin. Cancer Res. 41 (2022) 277, https://doi.org/10.1186/s13046-022-02486-z.
[45] C.J. de Witte, J. Espejo Valle-Inclan, N. Hami, K. Lõhmussaar, O. Kopper, C.P. H. Vreuls, G.N. Jonges, P. van Diest, L. Nguyen, H. Clevers, W.P. Kloosterman, E. Cuppen, H.J.G. Snippert, R.P. Zweemer, P.O. Witteveen, E. Stelloo, Patient-derived ovarian cancer organoids mimic clinical response and exhibit heterogeneous Inter- and intrapatient drug responses, Cell Rep. 31 (2020) 107762, https://doi.org/10.1016/j.celrep.2020.107762.
[46] J. Bi, A.M. Newtson, Y. Zhang, E.J. Devor, M.I. Samuelson, K.W. Thiel, K.K. Leslie, Successful patient-derived organoid culture of gynecologic cancers for disease modeling and drug sensitivity testing, Cancers 13 (2021), https://doi.org/10.3390/cancers13122901.
[47] S.J. Hill, B. Decker, E.A. Roberts, N.S. Horowitz, M.G. Muto, M.J. Worley, C. M. Feltmate, M.R. Nucci, E.M. Swisher, H. Nguyen, C. Yang, R. Morizane, B. S. Kochupurakkal, K.T. Do, P.A. Konstantinopoulos, J.F. Liu, J.V. Bonventre, U. A. Matulonis, G.I. Shapiro, R.S. Berkowitz, C.P. Crum, A.D. D'Andrea, Prediction of DNA repair inhibitor response in short-term patient-derived ovarian cancer organoids, Cancer Discov. 8 (2018) 1404–1421, https://doi.org/10.1158/2159-8290.CD-18-0474.
[48] M. Tao, F. Sun, J. Wang, Y. Wang, H. Zhu, M. Chen, L. Liu, L. Liu, H. Lin, X. Wu, Developing patient-derived organoids to predict PARP inhibitor response and explore resistance overcoming strategies in ovarian cancer, Pharm. Res. 179 (2022), https://doi.org/10.1016/j.phrs.2022.106232.
[49] A.E. Arias-Diaz, M. Ferreiro-Pantin, J. Barbazan, E. Perez-Beliz, J. Ruiz-Bañobre, C. Casas-Arozamena, L. Muinelo-Romay, R. Lopez-Lopez, A. Vilar, T. Curiel, M. Abal, Ascites-Derived organoids to depict platinum resistance in gynaecological serous carcinomas, Int J. Mol. Sci. 24 (2023) 13208, https://doi.org/10.3390/ijms241713208.
[50] E.A. Farshadi, J. Chang, B. Sampadi, M. Doukas, F. Van 't Land, F. van der Sijde, E. E. Vietsch, J. Pothof, B.G. Koerkamp, C.H.J. van Eijck, Organoids derived from neoadjuvant FOLFIRINOX patients recapitulate therapy resistance in pancreatic ductal adenocarcinoma, Clin. Cancer Res. 27 (2021) 6602–6612, https://doi.org/10.1158/1078-0432.CCR-21-1681.
[51] R. Wegmann, L. Bankel, Y. Festl, K. Lau, S. Lee, F. Arnold, V. Cappelletti, A. Fehr, P. Picotti, K.J. Dedes, D. Franzen, D. Lenggenhager, P.K. Bode, M. Zoche, H. Moch, C. Britschgi, B. Snijder, Molecular and functional landscape of malignant serous effusions for precision oncology, Nat. Commun. 15 (2024) 8544, https://doi.org/10.1038/s41467-024-52694-8.
[52] X. Sheng, J. Li, L. Yang, Z. Chen, Q. Zhao, L. Tan, Y. Zhou, J. Li, Promoter hypermethylation influences the suppressive role of maternally expressed 3, a long non-coding RNA, in the development of epithelial ovarian cancer, Oncol. Rep. 32 (2014) 277–285, https://doi.org/10.3892/or.2014.3208.
[53] E.A. Braga, A.M. Burdennyy, L.A. Uroshlev, D.M. Zaichenko, E.A. Filippova, S. S. Lukina, I.V. Pronina, I.R. Astafeva, M.V. Fridman, T.P. Kazubskaya, V.I. Loginov, A.A. Dmitriev, A.A. Moskovtsev, N.E. Kushlinskii, Ten hypermethylated lncRNA genes are specifically involved in the initiation, progression, and lymphatic and peritoneal metastasis of epithelial ovarian cancer, Int. J. Mol. Sci. 25 (2024) 11843, https://doi.org/10.3390/ijms252111843.
[54] M. Hayashi-Okada, S. Sato, K. Nakashima, T. Sakai, T. Tamehisa, T. Kajimura, I. Tamura, K. Sueoka, N. Sugino, Identification of long noncoding RNAs downregulated specifically in ovarian high-grade serous carcinoma, Reprod. Med. Biol. 23 (2024), https://doi.org/10.1002/rmb2.12572.
[55] Y. Li, S. Lou, J. Zhang, S. Zhao, G. Lou, m6A methylation-mediated regulation of LncRNA MEG3 suppresses ovarian cancer progression through miR-885-5p and the VASH1 pathway, J. Transl. Med. 22 (2024) 113, https://doi.org/10.1186/s12967-024-04929-x.
[56] Y. Li, L. Zhang, Y. Zhao, H. Peng, W. Bai, N. Zhang, MEG3 sponges miRNA-376a and YBX1 to regulate angiogenesis in ovarian cancer endothelial cells, Heliyon 9 (2023) e13204, https://doi.org/10.1016/j.heliyon.2023.e13204.
[57] Y. Liu, Y. Xu, L. Ding, L. Yu, B. Zhang, D. Wei, LncRNA MEG3 suppressed the progression of ovarian cancer via sponging miR-30e-3p and regulating LAMA4 expression, Cancer Cell Int. 20 (2020) 181, https://doi.org/10.1186/s12935-020-01259-y.
[58] L. Wang, M. Yu, S. Zhao, lncRNA MEG3 modified epithelial-mesenchymal transition of ovarian cancer cells by sponging miR-219a-5p and regulating EGFR, J. Cell Biochem. 120 (2019) 17709–17722, https://doi.org/10.1002/jcb.29037.
[59] Y. Xiu, K. Sun, X. Chen, S. Chen, Y. Zhao, Q. Guo, Z.-H. Zong, Upregulation of the lncRNA Meg3 induces autophagy to inhibit tumorigenesis and progression of epithelial ovarian carcinoma by regulating activity of ATG3, Oncotarget 8 (2017) 31714–31725, https://doi.org/10.18632/oncotarget.15955.
[60] Y. Zhou, X. Zhang, A. Klibanski, MEG3 noncoding RNA: a tumor suppressor, J. Mol. Endocrinol. 48 (2012) R45–R53, https://doi.org/10.1530/JME-12-0008.
[61] S. Ghafouri-Fard, M. Taheri, Maternally expressed gene 3 (MEG3): a tumor suppressor long non coding RNA, Biomed. Pharmacother. 118 (2019) 109129, https://doi.org/10.1016/j.biopha.2019.109129.
[62] Y. Zhou, H. Yang, W. Xia, L. Cui, R. Xu, H. Lu, D. Xue, Z. Tian, T. Ding, Y. Cao, Q. Shi, X. He, LncRNA MEG3 inhibits the progression of prostate cancer by facilitating H3K27 trimethylation of EN2 through binding to EZH2, J. Biochem. 167 (2020) 295–301, https://doi.org/10.1093/jb/mvz097.
[63] S.H. Malgundkar, Y. Tamimi, The pivotal role of long non-coding RNAs as potential biomarkers and modulators of chemoresistance in ovarian cancer (OC), Hum. Genet. 143 (2024) 107–124, https://doi.org/10.1007/s00439-023-02635-0.
[64] D.-Q. Li, Y.-R. Ding, J.-H. Che, Z. Su, W.-Z. Yang, L. Xu, Y.-J. Li, H.-H. Wang, W.-Y. Zhou, Tumor suppressive lncRNA MEG3 binds to EZH2 and enhances CXCL3 methylation in gallbladder cancer, Neoplasma 69 (2022) 538–549, https://doi.org/10.4149/neo_2022_210726N1046.
[65] R. Margueron, D. Reinberg, The polycomb complex PRC2 and its mark in life, Nature 469 (2011) 343–349, https://doi.org/10.1038/nature09784.
[66] H. Gujar, D. Weisenberger, G. Liang, The roles of human DNA methyltransferases and their isoforms in shaping the epigenome, Genes 10 (2019) 172, https://doi.org/10.3390/genes10020172.
[67] J. Zhang, J. Liu, X. Xu, L. Li, Curcumin suppresses cisplatin resistance development partly via modulating extracellular vesicle-mediated transfer of MEG3 and miR-214 in ovarian cancer, Cancer Chemother. Pharm. 79 (2017) 479–487, https://doi.org/10.1007/s00280-017-3238-4.
[68] N. Jin, T.L. George, G.A. Otterson, C. Verschraegen, H. Wen, D. Carbone, J. Herman, E.M. Bertino, K. He, Advances in epigenetic therapeutics with focus on solid tumors, Clin. Epigenet. 13 (2021) 83, https://doi.org/10.1186/s13148-021-01069-7.
[69] C. Li, Y. Wang, Y. Gong, T. Zhang, J. Huang, Z. Tan, L. Xue, Finding an easy way to harmonize: a review of advances in clinical research and combination strategies of EZH2 inhibitors, Clin. Epigenet. 13 (2021) 62, https://doi.org/10.1186/s13148-021-01045-1.
[70] A.M. Oza, U.A. Matulonis, A.A. Secord, J. Nemunaitis, L.D. Roman, S.P. Blagden, S. Banerjee, W.P. McGuire, S. Ghamande, M.J. Birrer, G.F. Fleming, M.J. Markham, H.W. Hirte, D.M. Provencher, B. Basu, R. Kristeleit, D.K. Armstrong, B. Schwartz, P. Braly, G.D. Hall, K.P. Nephew, S. Jueliger, A. Oganesian, S. Naim, Y. Hao, H. Keer, M. Azab, D. Matei, A randomized phase II trial of epigenetic priming with guadecitabine and carboplatin in Platinum-resistant, recurrent ovarian cancer, Clin. Cancer Res. 26 (2020) 1009–1016, https://doi.org/10.1158/1078-0432.CCR-19-1638.
[71] S. Chen, P. Xie, M. Cowan, H. Huang, H. Cardenas, R. Keathley, E.J. Tanner, G. F. Fleming, J.W. Moroney, A. Pant, A.M. Akasha, R.V. Davuluri, M. Kocherginsky, B. Zhang, D. Matei, Epigenetic priming enhances antitumor immunity in platinum-resistant ovarian cancer, J. Clin. Investig. 132 (2022), https://doi.org/10.1172/JCI158800.
[72] B.A. Jones, S. Varambally, R.C. Arend, Histone methyltransferase EZH2: a therapeutic target for ovarian cancer, Mol. Cancer Ther. 17 (2018) 591–602, https://doi.org/10.1158/1535-7163.MCT-17-0437.
[73] J. Chen, J.H. Hong, Y. Huang, S. Liu, J. Yin, P. Deng, Y. Sun, Z. Yu, X. Zeng, R. Xiao, J.Y. Chan, P. Guan, Y. Wang, P. Wang, L. Liu, S. Wen, Q. Yu, C.K. Ong, B.-T. Teh, Y. Xiong, J. Tan, EZH2 mediated metabolic rewiring promotes tumor growth independently of histone methyltransferase activity in ovarian cancer, Mol. Cancer 22 (2023) 85, https://doi.org/10.1186/s12943-023-01786-y.
[74] L.H. Jensen, S.R. Rogatto, J. Lindebjerg, B. Havelund, C. Abildgaard, L.M. do Canto, C. Vagn-Hansen, C. Dam, S. Rafaelsen, T.F. Hansen, Precision medicine applied to metastatic colorectal cancer using tumor-derived organoids and in-vitro sensitivity testing: a phase 2, single-center, open-label, and non-comparative study, J. Exp. Clin. Cancer Res. 42 (2023), https://doi.org/10.1186/s13046-023-02683-4.
[75] S.N. Ooft, F. Weeber, L. Schipper, K.K. Dijkstra, C.M. McLean, S. Kaing, J. van de Haar, W. Prevoo, E. van Werkhoven, P. Snaebjornsson, L.R. Hoes, M. Chalabi, D. van der Velden, M. van Leerdam, H. Boot, C. Grootscholten, A.D.R. Huitema, H. J. Bloemendal, E. Cuppen, E.E. Voest, Prospective experimental treatment of colorectal cancer patients based on organoid drug responses, ESMO Open 6 (2021) 100103, https://doi.org/10.1016/j.esmoop.2021.100103.
[76] W. Chen, P.-H. Fang, B. Zheng, Y. Liang, Y. Mao, X. Jiang, Q. Tang, Effective treatment for recurrent ovarian cancer guided by drug sensitivity from Ascites-Derived organoid: a case report, Int. J. Women's. Health 15 (2023) 1047–1057, https://doi.org/10.2147/IJWH.S405010.